Mohamed Khider University of Biskra
Faculty of exact sciences and natural and life sciences
Material sciences department

MASTER MEMORY

Material Sciences
Physics
Energetic Physics and Renewable Energies

Ref. :

Presented by:
SARRADJ AYMEN ABD EL OUADOUD

Le : 26/6/2022

Study of Silicon-Graphene solar cells by Simulation

Jury:

M^{me}	Boudib Ouahiba	MCB	Mohamed Khider University of Biskra	President
M^{r}	Boumaraf Rami	MCB	Mohamed Khider University of Biskra	Supervisor
M^{me}	Laiadi Widad	MCA	Mohamed Khider University of Biskra	Examiner

Academic Year: 2021/2022

ACKNOWLEDGEMENT

First of all, I thanks "**Allah**" for my success

I would like to express my sincerest gratitude and thanks to my supervisor **Dr Boumaraf Rami** for his invaluable guidance , generous support and great patience and encouragement not only for how to conduct research but also for how to be a researcher.

My sincere appreciation goes also to **University Mohamed Khider de Biskra** (Faculty of Exact Sciences and Sciences of Nature and Life /Matter Sciences Department) for providing me scholarships and access to various research instruments/facilities

I would not forget to thank the members of the jury, **Boudib Ouahiba** and **Laiadi Widad** who have kindly accepted to read and examine our work.

I am graceful to all my friends both in Constantine and Biskra for their help and support

Finally, I would like to express my deepest love and gratitude to my **family** especially my **parents** for their generous support, and great encouragement through my master degree and entire life.

ABSTRAT

The efforts to improve the efficiency of solar cells and the reduction of their costs have been a major concern for a long time.

Graphene, as a two-dimensional material with high electrical conductance, high transparency and flexibility make it used in many applications such as solar cells.

In this work we used SILVACO ATLAS software simulation to apply some improvements to graphene/Si solar cells such as adding interlayers, change their thickness and doping concentration, it seems that they can affects the efficiency and improves it from 2.27% to 5.63% in the best conditions.

ملخص

تعتبر الجهود المبذولة لتحسين كفاءة الخلايا الشمسية وتقليل تكاليفها مصدر اهتمام كبير منذ فترة طويلة.

الجرافين كمادة ثنائية الأبعاد ذات التوصيل الكهربائي العالي والشفافية العالية والمرونة تجعله يستخدم في العديد من التطبيقات منها الخلايا الشمسية.

في هذا العمل، استخدمنا المحاكاة بواسطة برنامج SILVACO ATLAS لتطبيق بعض التحسينات على خلايا graphene/Si الشمسية مثل إضافة طبقات بينية وتغيير سمكها وتركيز التطعيم، فتمكنا من تحسين الكفاءة من 2.27٪ إلى 5.63٪ في أفضل الظروف.

RESUME

Les efforts pour améliorer l'efficacité des cellules solaires et la réduction de leurs coûts sont depuis longtemps une préoccupation majeure.

Le graphène, tant qu'un matériau bidimensionnel à haute conductance électrique, haute transparence et flexibilité, fais-le utilisé dans nombreuses applications telles que les cellules solaires.

Dans ce travail, nous avons utilisé la simulation avec logiciel SILVACO ATLAS pour appliquer certaines améliorations aux cellules solaires de graphène/Si telles que l'ajout des couches intermédiaires, la modification de leur épaisseur et de changé la concentration du dopage, nous avons réussi d'améliorer l'efficacité de 2,27 % à 5,63 % dans les meilleures conditions.

TABLE OF CONTENTS

Chapter 3 Results and discussion

LIST OF SYMBOLS

λ wavelength

υ frequency

h Planck's constant (6.626×10^{-34}J.s).

E_λ energy of photon

C the speed of light in vacuum (2.998×10^8 m/s)

AM Air Mass

L_S the effective solar radiation path length in the atmosphere

L_A is the thickness of the atmosphere

I_{ph} the photo-generated current

I_0 the reverse saturation current

q the elementary charge

v voltage

n the ideality factor

k the Boltzmann constant

T the absolute temperature

I_{sc} Short circuit current

G is the generation rate

L_n is the electron diffusion length

L_p is the hole diffusion length

W is the width of the depletion region

q is the absolute value of electron charge

V_{OC} Open-circuit voltage

E_g Energie de gap

FF Fill Factor

ɳ efficiency

QE The quantum efficiency

EQE External Quantum Efficiency

IQE Internal Quantum Efficiency

R_S the series resistance

R_{SH} is the shunt resistance

LIST OF FIGURE

LIST OF TABLES

Introduction

Introduction

Introduction

- **World Energy Consumption**

Since the widespread use of electricity, mankind's dependence upon it has grown exponentially. In 2010, the world produced over 20.2 trillion kilowatt-hours of electricity, and it is predicted to grow to 39.0 trillion kilowatt-hours by 2040 as compared with average growth of 1.4 percent per year for all delivered energy sources [1].

Electrical consumption is almost certainly set to rise year on year, but the methods by which this power is produced is far from certain. Over the recent decades, several issues have arisen which has changed our perception of electricity. The most important issues are concerned with the environment and depleted fuel reserves.

- **Renewable Energy**

The alternative to fossil fuels is renewable or nuclear energy. Renewables are a source of energy that is replenishable and therefore everlasting. Worldwide directives have begun to emerge putting pressure on individual governments to reduce their dependency on fossil fuels, thereby reducing carbon emissions.

It is important to note that nuclear energy is often included as a renewable energy source as it does not produce carbon emissions. Strictly speaking however, nuclear energy is not truly renewable as uranium is required, and estimated uranium reserves will only last for another 80 years at the current usage rate [2].

Safety issues that have recently come to light (with the Fukushima nuclear disaster) could affect this prediction as public concerns over the technology escalate.

- **Solar Energy**

Solar renewable energy is typically split into two classifications, generation of heat and generation of electricity; technically referred to as solar thermal and solar photovoltaics respectively. This work will focus upon the use of solar photovoltaics for direct production of electricity. In 1839, Edmund Becquerel discovered the photovoltaic effect [3]. which is the basic principle by which solar photovoltaic cells operate. A solar cell converts energy from sunlight into electricity. The electricity produced by the solar cell is in the form of direct current (DC). Direct DC electricity production is unique to solar cells, with other renewable technologies such as wind and hydro power generating alternating current (AC). A single solar cell typically produces a very low voltage and therefore it is common for many solar cells to be connected together in series to provide a more useful, higher voltage. When

Introduction

cells are connected together to form a larger array, the product is known as a solar module or panel. Solar cells also produce direct current which for some applications is ideal, although most domestic appliances use alternating current. To convert the direct current produced by solar cells into an alternating current an electrical device called an inverter is used. An array of panels connected to an inverter forms the basics of a solar PV system, which is typically what is installed in domestic applications.

The growth of the industry is due largely to two factors. Firstly the advantages of solar photovoltaics over other renewable technologies and secondly financial incentives offered by governments.

- Advantages of solar photovoltaics over other renewable technologies:

- Zero carbon emissions
- Can work anywhere exposed to sunlight
- Not as obtrusive as wind turbines
- Virtually maintenance free as there are no moving parts
- Modular solar panels are used which allow for easy assembly of various size systems from Watts to Mega Watts.
- Ease of building integration due to the various sizes, colours and flexibility
- Direct current (DC) generation allowing for simple battery storage systems.
- **Cost Vs Efficiency**

Wafer based silicon photovoltaics have dominated the photovoltaic industry since the very beginning of the solar cell market in the 1950's [4]. Other than wafer based crystalline cells, the rest of the terrestrial PV market is made up of thin film cells such as amorphous silicon (a-Si), cadmium -telluride (CdTe) and copper indium gallium selenide (CIGS) [5].

Despite the current market conditions, other cell technologies are predicted to gain a larger market share .

The commercial success of a solar cell technology not only relies upon efficiency but also the cost of producing the cell. Wafer based silicon solar cells dominate the market despite only being around 18-20% efficient. The reason they are so successful is that they provide reasonable electrical power at low cost. These parameters are critical for commercial installations of PV where people are competing directly against the cost of other renewable and fossil fuel technologies. For niche applications where cost is not as significant, high efficiency cells can be used for their higher electrical output, for example lll-V solar cells

Introduction

for satellite applications. Figure 1 shows the typical efficiency and cost implications of each of the solar cell generations.

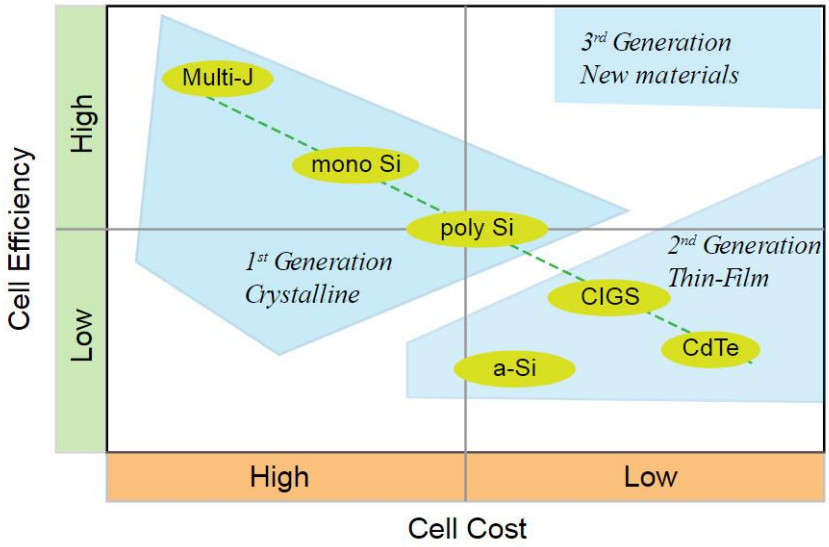

Figure 1 : Efficiency Cost Profile for different solar generations [6].

Despite the low efficiency of wafer based crystalline silicon cells compared to multijunction cells that can exhibit efficiencies in excess of 40%, silicon cells dominate the market place. The reason for the great success of silicon is due to its abundance of raw materials, reliability, ease of construction, and wealth of knowledge in the area taken from the semiconductor industry.

The focus of solar photovoltaics has always been strongly influenced by efficiency and cost. In order for the industry to continue to impact upon the renewable energy market, cell efficiency will need to rise or costs will need to reduce or preferably a combination of both. Unfortunately however, a trade-off currently exists between these two factors.

Chapter 1

Chapter 1 Principles of solar cells

1. Solar irradiation

The operation of the crystalline photovoltaic solar cell is based on the generation of the charge carriers due to the partial absorption of sunlight semiconductor materials.

Sunlight is an electromagnetic radiation which can be viewed as being composed of particles called photons. These photons convey a specific amount of energy determined by the spectral properties of their source.

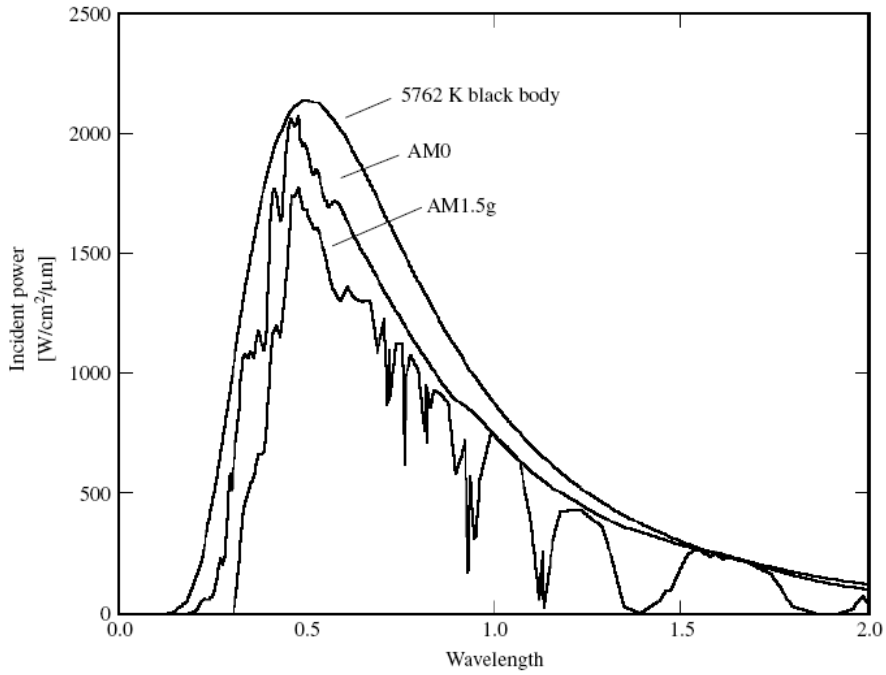

Figure 1.1: The radiation spectrum of a black body at 5762K compared with solar AM0 and AM1.5 global spectra [7].

The electromagnetic radiation can be characterized by wavelength (λ) and frequency (υ) or in terms of photons which characterised by energy ($h\upsilon$) expressed in electron volts where the energy carried by a single photon depends on its wavelength (E_λ).

The relation between these quantities are shown in the following equations:

$$\upsilon = \frac{C}{\lambda} \qquad (1.1)$$

$$\mathrm{E}_\lambda = \frac{hC}{\lambda} \qquad (1.2)$$

In Equations 1.1 and 1.2 , c is the speed of light in vacuum (2.998×10^8 m/s), where h is Planck's constant (6.626×10^{-34}J.s).

The sun possesses many properties that could be discussed extensively. However, the most important parameters for photovoltaic solar cells studies are the irradiance, the amount

power incidence on a surface per unit area, and the spectral characteristics of the light [8]. Figure 1.1 shows the spectral distributions of various sources of the light.

The irradiance value outside the Earth's atmosphere is called the solar constant, and it is equal to 1365 W/m2. However, once the irradiance enters the earth's atmosphere, it suffers from absorption losses due to the presence of molecules composing atmosphere such as ozone, oxygen, carbon dioxide and water vapor. Moreover ,aerosol and dust induce absorption losses nearly over the entire spectral range which leads to a global reduction of the incident power [9].

Therefore, the radiation on the earth's surface reaching a particular place is variable.

Also, other factors affect this variation including the daily and yearly variation due to the motion of the sun, local atmospheric conditions such as the sun. The mentioned conditions inuence the spectral component of the sunlight, the direct and the diffused components. The direct component of the solar irradiation is part of the sunlight that reaches the earth's surface directly whereas the diffused component is generated due to scattering of the sunlight in the atmosphere. Also, albedo could be presented to the total solar spectrum which refers to the reflected part of the solar irradiation from the earth's surface. The total solar radiation, also called global radiation, is composed of these three components.

The standard solar spectrum is normally referred as $AM1.5G$ where G stands for global sun and AM stands for Air Mass. It is determined by the angle of the incidence (θ), θ=0° when the sun is directly overhead; AM is defined in the Equation 1.3:

$$AirMass(number) = \frac{L_S}{L_A} = \frac{1}{cos\theta} \qquad (1.3)$$

Where L_S is the effective solar radiation path length in the atmosphere, L_A is the thickness of the atmosphere and also: the overhead path length of the light, vertical positioning of the sun for the angle of the incidence (θ) relative to the normal of the earth's surface and irradiation flux of 1000 W/m2 (=100 mW/cm^2 or 1 sun).

The AM factor refers to the information about absorption losses and changes to the spectrum due to absorption in the atmosphere before reaching the solar converter.

Therefore, it varies with the latitude and the time of the day and the year.

Chapter 1 Principles of solar cells

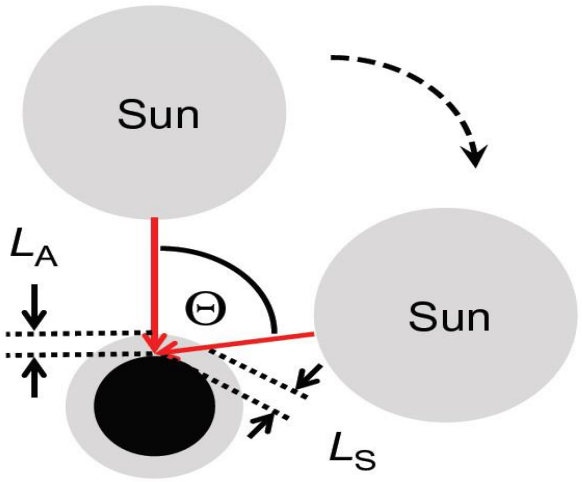

Figure 1.2: A sketch showing defnitions for AM factor [10].

The defnition of AM is given in figure 1.2 and equation 1.3.

The most commonly used AM factor values are:

- AM0: defines the extra-terrestrial spectrum at the boundary of the atmosphere which is the irradiance of 5800 K black body with intensity about 28% higher than M1.5G.
- AM1: measured at ground level for the sun at Zenith.
- AM1.5: correspond to an angle 48.2°. It is the standard for evaluation of the performance of solar panels. For solar concentrators, direct irradiation is used and the corresponding spectrum is $AM1.5D$, which is 10% less intense in comparison to $AM1.5G$.

Weather station can provide measurements of the solar irradiation, and historical data can be recorded. Solar radiation database is available to access by the US Department of Energy from EnergyPlus website [11]. Also, it can be obtained through Photovoltaic Geographical Information System (PVGIS) Website by Institute for Energy and Transport (IET) by the European Commission, which provides with a map-based inventory of solar energy resource [12]. Figure 1.3 illustrates an example of the average hourly radiation data for each month of the year for the location of Warsaw .

Irradiance data is an essential component of the weather files for the assessment of the electricity generation from photovoltaic systems. Despite the fact, that many weather/meteorological stations measure the received irradiation, solar radiation can be estimated with the knowledge of the local climate for a particular location using solar radiation models. These models vary in complexity and summaries of these approaches for the estimation for radiation data is given in [13, 14].

Chapter 1 Principles of solar cells

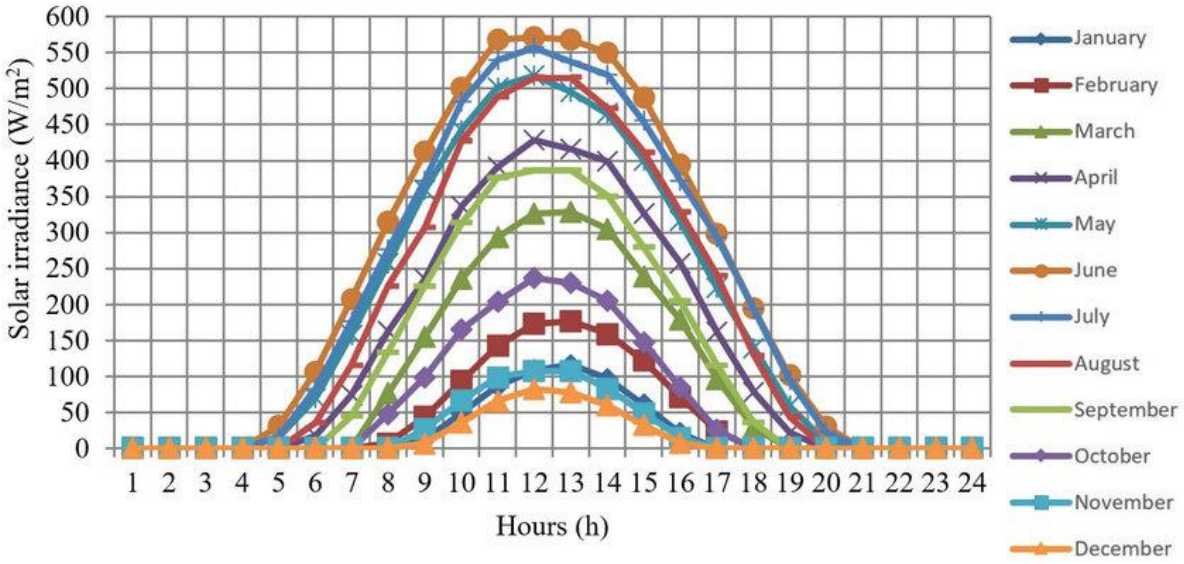

Figure 1.3:Average hourly radiation data for each month of the year in W/m2 in warsaw[15].

2. The P-N junction

Semiconductor solar cells rely upon the structure of a p-n junction. Due to the importance of the p-n junction, a brief description will be given. Since this work is related with silicon photovoltaics , examples which refer to Si p-n junctions will be given Semiconductor materials used for solar cell fabrication such as silicon are often pure crystalline materials.

Silicon for example has four valence electrons which are shared with four neighbouring atoms forming covalent bonds. All the electrons are being utilized in covalent bonds and the material is at equilibrium, no excess electrons or holes. The material is referred to as an intrinsic semiconductor and contains no impurities or dopants.

Semiconducting materials are called such as they are able to conduct electricity above absolute zero. If the thermal energy is enough to overcome the band gap, an electron is promoted from the valence band to the conduction band where it is free to participate in conduction. The vacancy left by the electron is referred to as a hole which is positively charged. Both the electron and hole are able to participate in conduction and they are often referred to as electron hole pairs or carriers (as they carry charge). The larger the band gap of the material the harder it is for an electron to be thermally excited to the conduction band. Therefore the higher the band gap the more insulating a material becomes and the lower the band gap the more conducting it is. A semiconductor material is in between these two conductivities. It is very important to note that in an intrinsic semiconductor, few electrons are thermally excited and the material is only partially conductive. Elevating the temperature however can increase the number of electrons excited and therefore increase conduction in

the semiconductor. At 25 °C the intrinsic carrier concentration of silicon is 8.3 x $10^9 cm^{-3}$ while at 50°C it is 5.836 x $10^{10} cm^{-3}$ [16].

To produce a solar cell and utilize the photovoltaic effect, two differently charged semiconducting regions are required to form a p-n junction. This essentially involves creating a junction where one side has an increased amount of electrons available (n-type as electrons have negative charge) and the other has an excess of holes available (p-type as holes have positive charge). In an n-type material there are more electrons than holes and therefore the majority carriers are the electrons and the minority carriers are the holes.

In p-type, holes are majority carriers and electrons minority carriers.

In order to make an intrinsic semi-conducting material n or p-type, another element must be added which has atoms with excess electrons or excess holes. The addition of such a material is referred to as 'doping', where impurities are added to disrupt the intrinsic qualities of the semiconductor. Once again using silicon as an example, a material containing an excess electron is required to produce n-type silicon. From table 1.1, a group V material is required for n-type doping, such as Phosphorous. Similarly to produce p-type silicon a group III material is required, such as Boron.

III	IV	V
boron 5 B 10.811	carbon 6 C 12.011	nitrogen 7 N 14.007
aluminium 13 Al 26.982	silicon 14 Si 28.086	phosphorus 15 P 30.974
gallium 31 Ga 69.723	germanium 32 Ge 72.61	arsenic 33 As 74.922

Table 1.1: Group III to V o f the periodic table

Doping of a semiconductor such as silicon is typically carried out by diffusing a dopant into he material at high temperature. The material is first doped p or n-type during the silicon growth process, followed by a diffusion doping procedure to add in the other dopant layer.

The doping concentration, and the number of atoms introduced with free holes or electrons, strongly affects the number of majority and minority carriers. Alternative doping processes such as ion implantation can be used, but diffusion doping is the most commonly used method for silicon PV cells [17].

Now that a p-n junction has been created, the photovoltaic effect can be exploited.

Figure 1.4 below shows a typical schematic of the cross section of a silicon solar cell.

Chapter 1 Principles of solar cells

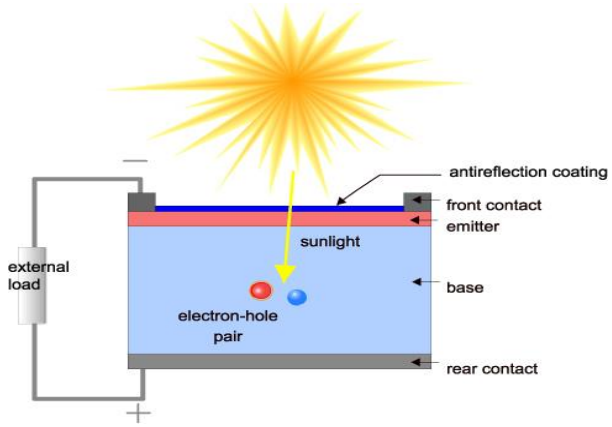

Figure 1.4: Cross section of a silicon solar cell [18].

Figure1.4 shows a p-n junction with a metal contact to the top n-type silicon (called the emitter), and an electrical contact to the bottom p-type material (called the base).

Since photons of energy from the sun must enter the cell, the front contact is made up of a series of gridlines/fingers which allow a proportion of the light to enter the cell whilst still making an electrical contact to the silicon. An antireflective layer is deposited onto the surface of the cell to reduce reflectivity by enhancing light capture.

When a photon from the sun is incident on the cell, if the energy of the photon is greater than or equal to that of the band gap of the semiconductor material, it is absorbed. For silicon that has a band gap of around 1.12eV, only photons with energy equal to 1.12eV or above will be utilized by the cell. Photons with energy less than the band gap will pass through the semiconductor without being absorbed. Photons with higher energy than that of the band gap can lose any energy higher than the band gap as heat and end up in the same position in the band gap as electrons excited by photons equal to the band gap.

When the photon energy is high enough and is absorbed, an electron is promoted from the valence band into the conduction band. The promotion creates a minority and majority carrier depending on the doping of the semiconductor. For a standard n-type emitter silicon solar cell, the minority carrier in the n-type emitter would be a hole.

Minority carriers can only exist for a short amount of time before they naturally recombine (energy wasted and not utilized by cell). The job of the p-n junction is to keep them apart prohibiting recombination (using an electric field) as shown in figure 1.5.

If the minority carrier (hole) makes it to the junction, the electric field created at the p-n junction transports it across the junction (to p-type silicon) where it is now a majority carrier

and can contribute to current flow . The electron in the emitter is now free to move out of the cell through the top electrical contact, dissipate its energy through the external load before re-entering the cell through the back contact w here it can recombine with the hole. Unfortunately not all minority carriers make it across the junction due to recombination mechanisms that exist in the bulk and at the surface of the cell. Any carriers that recombine are lost and no current can be generated from them . Thus, to maximise the efficiency of a cell, carriers should be generated in the vicinity of the p-n junction.

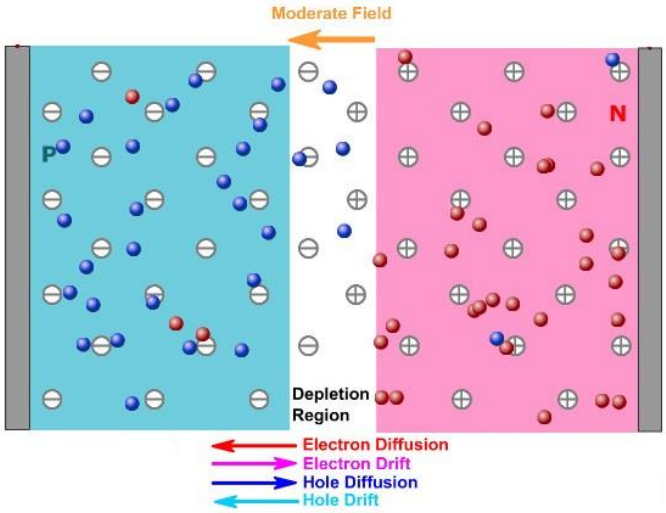

Figure 1.5: p-n junction of solar cells [19].

3. Type of solar cells

Photovoltaic solar cells are typically divided into three categories called generations, depending on the basic material used [20]:

- First Generation: Crystalline silicon.
- Second Generation: Thin film technologies.
- Third Generation: includes new concept devices.

Figure 1.6 shows a tree of PV technologies while the recorded efficiencies of solar cells and commercial PV modules are presented in table 1.2 and the time-line of the solar cell energy conversion efficiencies records is shown in figure 1.9

Chapter 1 Principles of solar cells

Generation	Technology	Efficiency (%) Cell	Module
1st	Mono-crystalline Silicon	25.6	22.9
	Multicrystalline Silicon	20.4	18.5
2nd	CIGS	20.5	15.7
	CdTe	19.6	17.5
	Amorphous Silicon	10.1	11.6
	Thin Film Polycrystalline Silicon	11.0	8.2
3rd	Multijunction	37.9	NA
	Organic	10.7	NA
	Dye Sensitised	11.9	NA

Table 1.2: Confirmed efficiencies of solar cells and commercial PV modules [21].

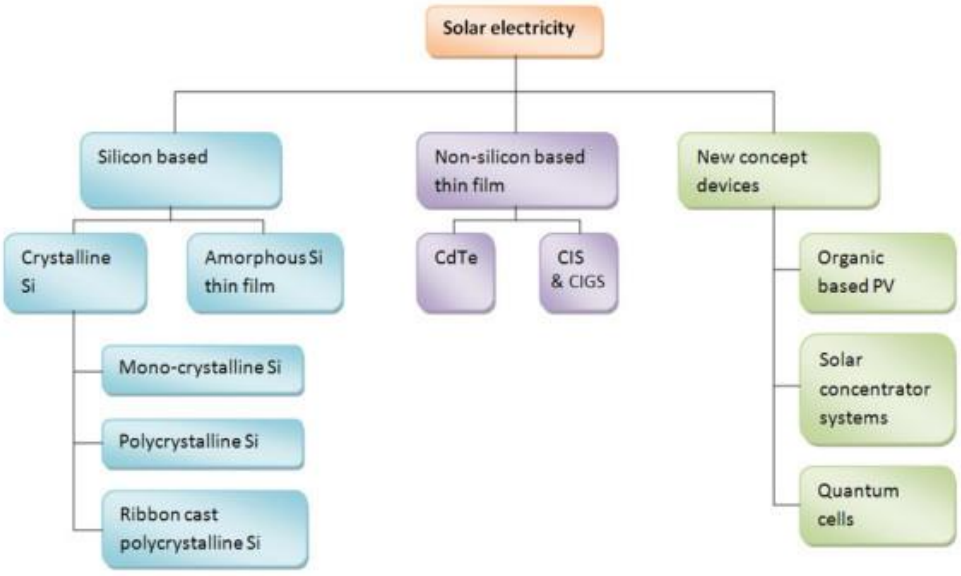

Figure 1.6: PV technologies tree [20] .

3.1. First Generation PV

The first generation includes solar cells that are relatively expensive to produce.

It includes mono-crystalline, multi-crystalline and ribbon silicon solar cells.

3.1.1. Monocrystalline Solar Cells

Monocrystalline silicon solar cells are produced from a single crystal silicon structure High purity silicon ingots are extracted from a cast then cut into thin wafers and then processed into PV cells. The corners of the cells are cropped because the silicon wafer is cut from cylindrical ingots which is grown by the Czochralski process.

The estimated life span of these solar cells is around 25-30 years [22].

Mono-crystalline silicon solar cells are expensive but more efficient than other type of solar cells. The highest recorded efficiency of mono-crystalline solar cells is 25.6% by Panasonic[21].

3.1.2. Multicrystalline Solar Cells

Production of multi-crystalline silicon solar cells is more economical and efficient in comparison to mono-crystalline solar cells. However, multi-crystalline solar cell have a lower efficiency than a mono-crystalline solar cell. In multi-crystalline silicon, the silicon is cast in blocks. When it hardens, it results in crystal structures of different sizes and exhibits defects which reduces the solar cell's efficiency .

The highest recorded efficiency of the multi-crystalline solar cell is 21.3% by Trina Solar [23].

3.1.3. Ribbon Solar Cells

Ribbon silicon cells are also called string ribbon cells. It is a type of multicrystalline silicon which is produced by extracting a flat thin film from molten silicon and results in a polycrystalline structure. This technique provides low-cost Si due to the high utilisation of the Si feedstock. Therefore, these cells are cheaper to make than multi-Si, due to a significant reduction in silicon waste but they are also less efficient.

3.2. Second Generation PV

The second generation covers types of solar cells with lower efficiency than the first generation but is much cheaper to manufacture. The second generation photovoltaic are often called thin-film solar cells because when compared to crystalline silicon-based cells they are made of layers of semiconductor materials that is only a few micrometers thick.

3.2.1. Amorphous Silicon Cells

The main difference between crystalline silicon and amorphous silicon (a-Si) that in the later, the silicon atoms are located at various distances from each other unlike crystalline and the angles between the Si-Si bonds do not have a unique value.

Amorphous silicon solar cells are incorporated with hydrogen which increases the photo-conductivity significantly while pure silicon exhibit poor optical and electrical properties [24]. It is important to mention that when the amorphous silicon solar cell is made of a p-n junction, the p and n material showed poor transport properties of electrons and the p-n junction amorphous silicon solar cell had low efficiency.

The p-i-n junction cell as shown in figure 1.7 was developed to enhance the poor transport properties. Unlike crystalline silicon cells which feature a grid contacts on the top surface,

the p-i-n amorphous silicon solar has a transparent conducting contact deposited as a thin film of Tin oxide of at the surface of the p+ layer and a metal contact is located at the rear of the cell [25].

The highest recorded effciency of amorphous silicon solar cells is 13.6% by AIST research centre for photovoltaic [23].

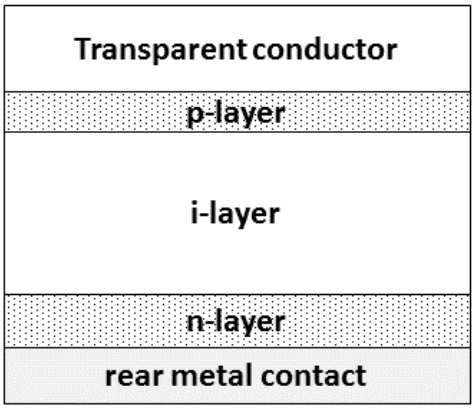

Figure 1.7: A schematic of amorphous silicon p-i-n solar cell structure.

3.2.2. Copper Indium Gallium Cells

Overall, elements from the group I, III, VI in the periodic table are of great potential for applications in photovoltaic and in particular for thin film solar cell application. Copper Indium Gallium Selenide (CIGS) cells are made with a thin layer of copper indium gallium diselenide Cu(In, Ga)Se2. CIGS solar cells are manufactured by the deposition of a thin layer of the following materials: copper, indium, gallium and selenide on a substrate of glass or plastic with electrodes collect the current on the front and back. The highest recorded efficiency of CIGS cells is 22.3% by Solar Frontier with similar durability as silicon solar cells. However, manufacturing costs CIGS solar cells are high when compared with amorphous silicon solar cells[21].

3.2.3. Cadmium Telluride Cells

Cadmium telluride (CdTe) solar cells are often produced using manufacturing processes such as screen-printing, galvanic disposition or spray pyrolysis can be used to produce the CdTe cells. The structure of CdTe solar cells consists of a glass substrate with a transparent conduction layer and an indium tin oxide (ITO) coated front contact cover which is sandwiched with Cadmium Sulphide (CdS) to form a p-n junction photovoltaic solar cell. Typically, CdTe cells use an n-i-p structure. However, Large-scale of CdTe modules can be achieved through a vapour deposition process.

First Solar announced achieving a record 22.1% conversion efficiency in their CdTe cells [21].

3.3. Third Generation PV

The term third generation is used to describe solar cells that are very efficient.

Most technologies in this generation are not yet commercial, but there is an extensive research is being carried out in this area.

3.3.1. Dye Sensitised and Organic cells

The primary material of a Dye Sensitised Solar Cells (DSSCs) is the semiconductor titanium dioxide. In comparison to p-n junction cells, dye-sensitised cells have a different mode of function. Light absorption occurs at a very specific location in the dye molecules which covers a porous layer of titania nanoparticles [26].

Most of the materials for DSSCs are non-toxic and inexpensive to produce.

DSSCs are attractive as a replacement for "low-density" applications like rooftop solar collectors, where the light weight of the glass-less collector is a significant advantage.

The main disadvantage to the design of DSSCs is the use of the liquid electrolyte, which results in temperature stability Issues. At low temperatures, the electrolyte can freeze, terminating the generation of power while at higher temperatures can cause the liquid to expand, making sealing the panels a serious problem. Dye-sensitised cells are tolerant to poor incidence angles and shading with solar to electrical conversion efficiency increasing at higher temperatures in contrast to crystalline silicon cells. The highest reported DSSC efficiency achieved to date was 11.9% by Sharp [23]. Due to the compatibility of solution-processible organic semiconductors with printing-based production and low-cost, flexible substrates, organic cells offer a substantial potential for photovoltaic systems in the future. Materials of particular interests are molecular, and polymeric semiconductors and fullerene (C60) and its derivatives are attractive materials for the development of organic cells [27].

However, they still do not achieve the requirements of practical applications. The highest achieved efficiency reported for organic cells to date by Hong Kong UST who achieved an efficiency of 11.5% [23].

3.3.2. Perovskite Solar Cell

Perovskite solar cells have attracted a noticeable attention in a short period.

The conversion efficiency of perovskite solar cells improved from under 4% in 2010 to 22% in 2016. Perovskite solar cells features a high absorption coefficient with a thickness of

around 500 nm to absorb solar energy, but perovskite solar cell degrades quickly in a moist environment [28].

The perovskite structure can be defined as any compound that has the generic form ABX3 and the same crystallographic structure as perovskite mineral. Perovskite can be illustrated as a large positively charged atomic or molecular cation of type A in the centre of a cube. Also, positively charged cations have occupied on the corners of the cube represented as atoms B where a smaller atom X occupies the faces of the cube with a negative charge. The most efficient perovskite solar cells so far have been produced with the following combination of materials in the usual perovskite form ABX3: A = an organic cation - methylammonium, B = a big inorganic cation - typically lead, and X3= a slightly smaller anion typically chloride or iodide.

Figure 1.8 shows a schemat of Perovskite solar cell where a perovskite solar cells can be integrated very easily into a standard organic PV or other thin film architecture

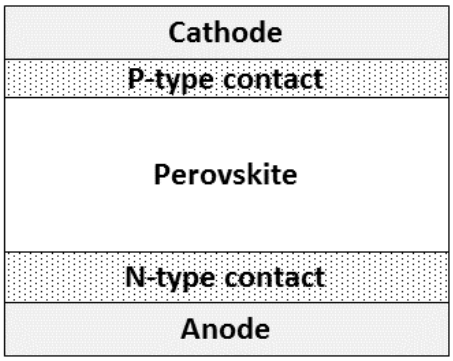

Figure 1.8: A schemat of the structure of Pervoskite solar cell.

Chapter 1 Principles of solar cells

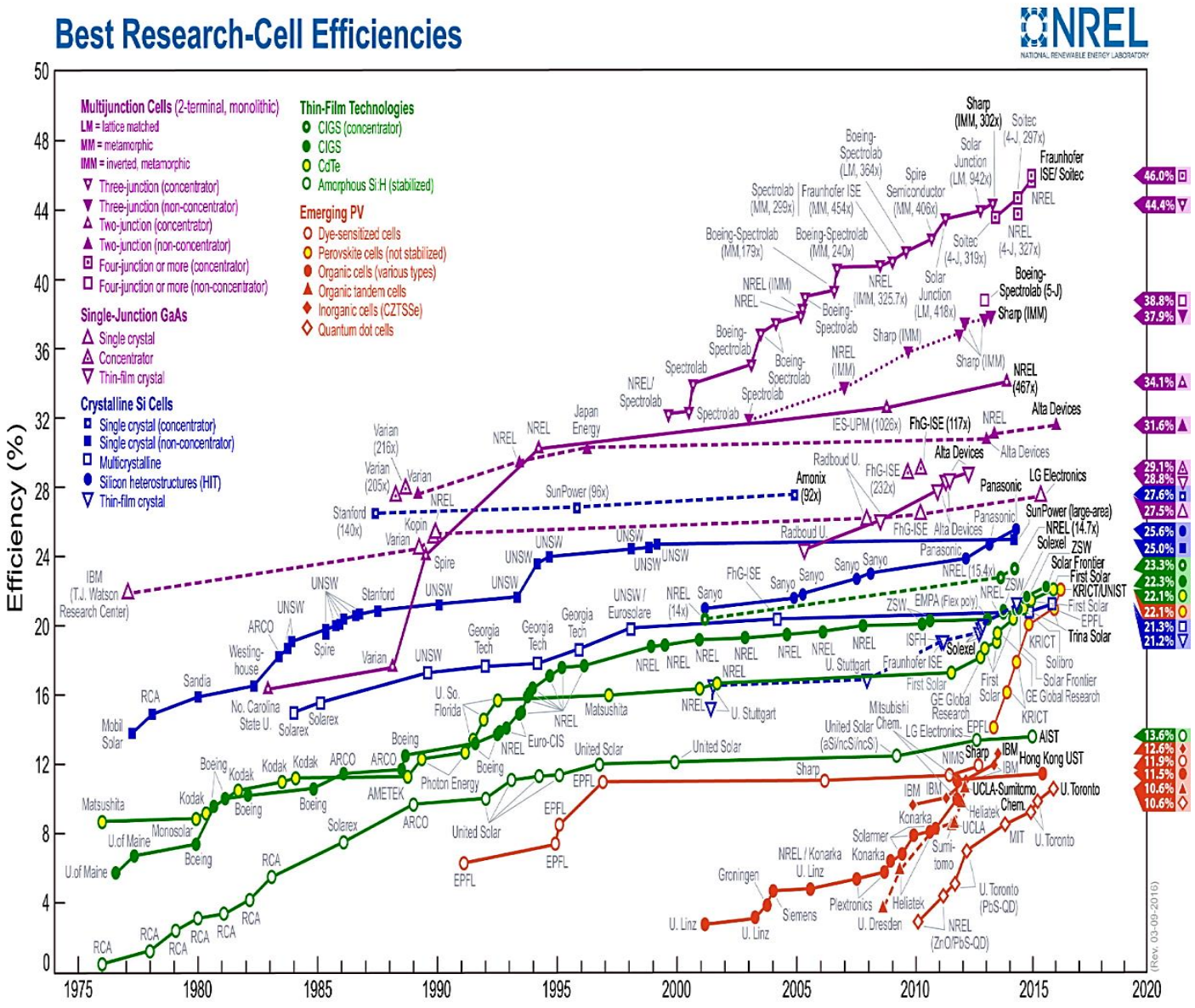

Figure 1.9: Timeline of solar cell energy conversion effeciencies records [23].

4. Principles of Solar Cells Operation

The concept of energy conversion of the p-n junction solar cells can be summarized as follow A photovoltaic solar cell is an electronic device that can convert sunlight into electricity directly. Exposing the solar cell into light produces both current and voltage which enerate electrical power. This process, called photovoltaic effect, requires a material where its absorption of the light excites an electron to a higher energy state and then extract it from the solar cell into an external load where it dissipates its energy in the external circuit and returns to the solar cell. In general, the majority of the photovoltaic devices need an internal electric field that leads to the separation of the photo-generated charge carriers (electrons and holes) where this separation occurs at the p-n junction of the PV cell.[29,30] .

Figure 1.10 represents the common design pattern of the single p-n junction crystalline solar cells (mono or multi-crystalline silicon wafer), with a crystalline silicon wafer 200-300 micron thick [31]. The electrical contacts in the cell are the front grid and back contact. The front metallic grid pattern is designed in a way to maximize the collection of photo-generated current by reducing the coverage of the front surface of the cell by widely spacing the grid to allow the light to enter the cell but not extent to raise a struggle for the fingers to collect the current produced by the cell. On the other side of the cell, these restrictions do not apply to the rear metallic contact layer which serves only as a metallic contact. The silicon wafer reflects 30% of the incident light on the cell [32]. Therefore, an anti-reflection coating is applied to the front surface of the solar cell to minimise the reflection losses from the top surface of the wafer and increase the amount of light absorbed by the cell which leads to improving the conversion efficiency of the silicon solar cell.

Silicon nitride is commonly used as an anti-reflection layer for commercial silicon

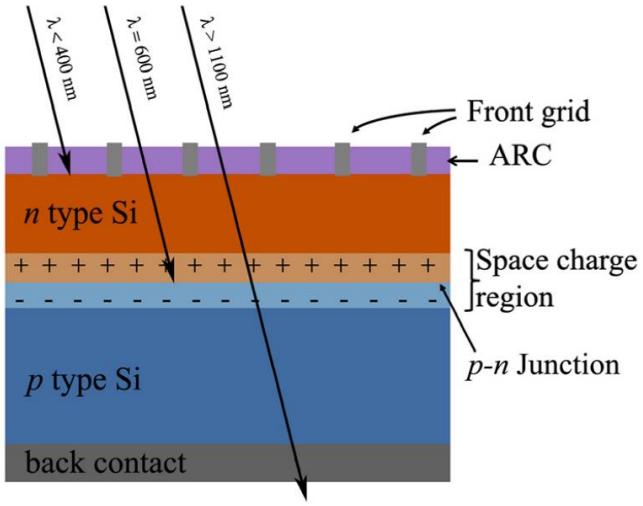

Figure 1.10: Architecture of a p-n junction Si solar cell [31].

solar cells due to its excellent passivation properties that prevent carrier recombination at the surface of the solar cell. Silicon nitride is deposited on the solar cell as a thin film with a thickness of about 80 nm using PECVD [31].

5. Characteristic of C-Si Solar Cell

. An ideal solar cell can be represented as a diode connected in parallel with a light controlled current source as shown in figure 1.11 [33, 34].

Chapter 1 Principles of solar cells

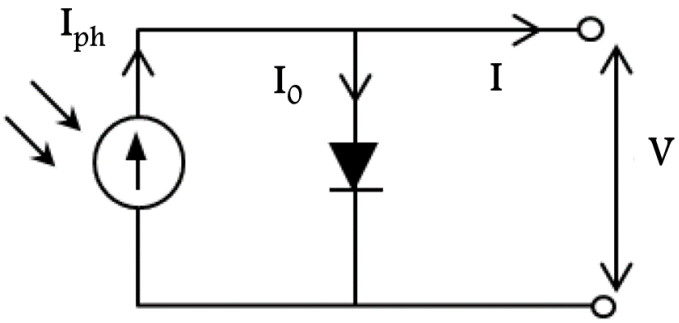

Figure 1.11: The equivalent circuit model of an ideal solar cell.

The performance of crystalline silicon solar cells is evaluated by current-voltage (I-V) measurement. Based on the standard diode equation, I-V characteristics of a single junction solar cell under illumination can be written as the linear superposition of the I-V curve of the solar cell diode in the dark with the light-generated current [25].

$$I = I_{ph} - I_0\left(e^{(\frac{qv}{nkT})} - 1\right) \qquad (1.4)$$

Where I_0 is the reverse saturation current, q is the elementary charge, T the absolute temperature and n the ideality factor ($n = 1$ for ideal p-n junction where the current is dominated by diffusion mechanism whereas $n = 2$ when the current is dominated by the recombination phenomena in the space charge region), k the Boltzmann constant, I_{ph} is the photo-generated current. When the PV cell is not illuminated (dark condition), there are no contributions from the photo-generated current and the resulting diode characteristic curve is shown in figure 1.12. By illuminating the PV cell, reported in the same figure, the dark curve is shifted down into the fourth quadrant by the current I_{ph} where the power can be extracted from the cell, the output of the solar cell is characterized using four main parameters:

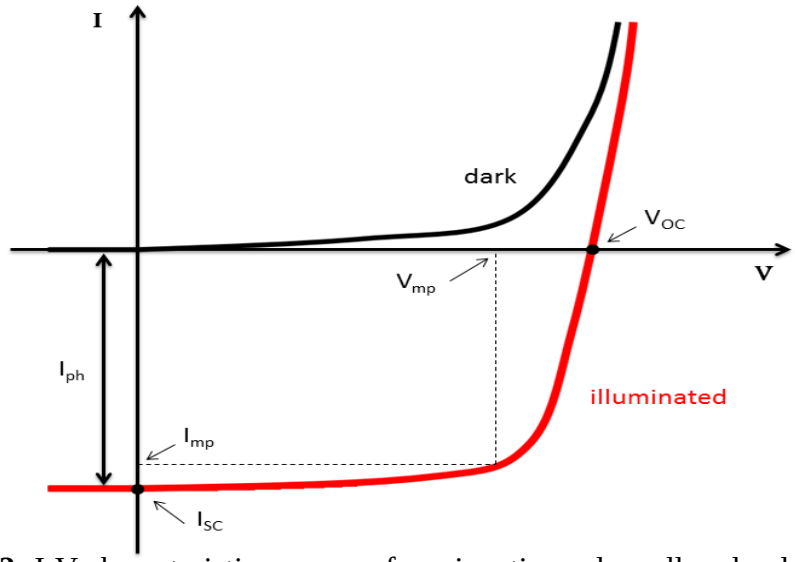

Figure 1.12: I-V characteristics curves of p-n junction solar cell under dark and light illumination conditions [25].

Chapter 1 Principles of solar cells

5.1. Short circuit current (I_{sc}):

Is current that can be reached through the solar cell under illumination when the voltage across the solar cell is zero. (when the PV device is short-circuited. In other words, when the terminals of the PV device are connected with each other). Ideally, this parameter is equal to the light-generated current under illumination (I_{ph}).

The short circuit current of a solar cell relies upon two factors, the electron-hole pair generation rate and the collection probability (successfully collecting light generated carriers).

1. The amount of light generated carriers is in turn dependent on several aspects.

Major aspects include:

• Band-gap of the solar cell: Only photons entering the cell with a higher energy than that of the band gap will contribute towards current generation. Photons must have enough energy to be able to excite an electron from the valence to the conduction band (electron-hole pair generated). For example, a silicon solar cell with a band gap of 1.12eV requires wavelengths shorter than 1100nm. There0fore the spectrum of light incident on a cell is of high importance.

• Light intensity: A higher light intensity would mean a higher I_{sc} as there is more irradiative power per unit area.

• Reflectivity of the solar cell material: If the surface of the material has a high reflectivity, photons can be reflected away and not utilized. The lower the reflectivity the more light enters the cell, rather than being lost by reflection.

• Absorption coefficient of the cell material: Essentially a measurement of how good a material is at absorbing a photon. Some wavelengths get absorbed at the surface of a cell material and others deeper into it. A high absorption coefficient is advantageous. Different semiconductors have different coefficients.

• Thickness of cell: different wavelengths get absorbed (utilized for current generation) at different depths in a semiconducting material. If the material is too thin, photons can pass through it without being absorbed.

2. The collection probability is the likelihood that a light generated carrier will make it to the p-n junction and therefore be utilized for current generation. Unfortunately due to recombination mechanisms and other losses, not every carrier generated will contribute to power generation. Collection probability relies upon:

• Recombination mechanisms: If a carrier recombines before it makes it to the depletion region it no longer contributes to power generation as it loses its energy usually as heat. For indirect materials such as silicon, recombination is typically caused by defects at the surface or within the material. Different recombination mechanisms exist for the surface of the material than that of the bulk.

• The distance away from the depletion region a carrier is generated: If a carrier is generated within the depletion region then the probability of it being collected will be100%.

The region where carriers can be collected successfully is roughly within a diffusion length of the p-n junction. Further away from the depletion region, the probability decreases as the distance carriers must travel is larger. Therefore the probability of recombination is higher. From the factors that affect short circuit current mentioned above, it is surmised that Isc is the same as that of the current produced by light generation. Unfortunately further losses occur due to the collection of light generated carriers by the electrical contacts to the solar cell (resistive loss mechanisms).

From the two main factors that make up the I_{sc}, the simplified equation (neglecting recombination and assuming uniform generation) for a solar cell short circuit current is:

$$I_{sc} = qG(L_n + L_p + W) \qquad (1.5)$$

Where:

G is the generation rate

L_n is the electron diffusion length

L_p is the hole diffusion length

W is the width of the depletion region

q is the absolute value of electron charge

5.2. Open-circuit voltage (V_{OC}):

Is the maximum voltage available from a solar cell established under illumination, and this occurs when the current through the PV device is zero, (when the circuit is not closed).

V_{OC} can be calculated from equation 1.4 with the condition $I = 0$:

$$V_{OC} = \frac{nkT}{q} ln\left(\frac{I_{ph}}{I_0} + 1\right) \qquad (1.6)$$

The open circuit voltage is thus an indicator to the amount of recombination in the cell. A material with a large band gap has a lower minority carrier concentration and therefore the chances of recombination are lower. Therefore a cell with a larger band gap can have a larger open circuit voltage. This is demonstrated in figure 1.13. silicon (Eg of 1.12eV) has a

maximum V_{OC} of 0.7V. Such a high open circuit voltage would be found using high purity silicon substrates.

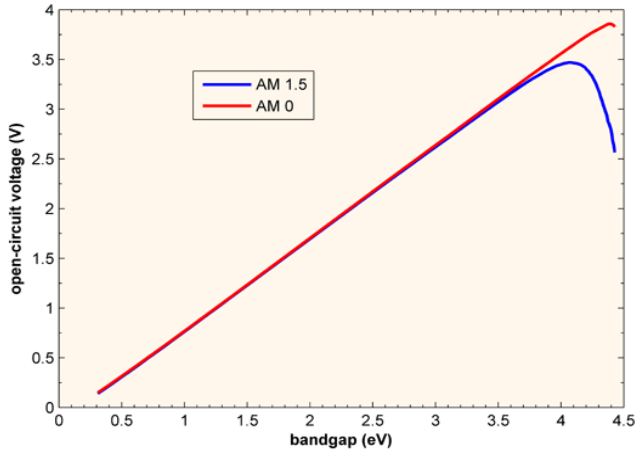

Figure 1.13: Open circuit voltage with respect to band gap energy

5.3. Fill Factor (*FF*):

Is a measure of the squareness of the solar cell characteristics and it is defined as:

$$FF = \frac{I_m V_m}{I_{sc} V_{OC}} \qquad (1.7)$$

Where (I_m , V_m) is a particular operating point, corresponding to the maximum power output. Graphically, The higher FF, the higher power that can be extracted from the cell.

An ideal solar cell should have a *FF*=1 (100%), however the effects of parasitic series and shunt resistances and other non-idealities can reduce this quantity .

5.4. efficiency η

Energy conversion efficiency is defined as:

$$\eta = \frac{P_{out}}{p_{in}} = \frac{I_m V_m}{GA} = \frac{I_{sc} V_{OC}.FF}{GA} \qquad (1.8)$$

Where G is the incident solar radiation and A is the effective solar cell area which represents the illuminated area of the solar cell. The efficiency of the device depends on the parameters I_{sc} , V_{OC} and FF where the higher values of these parameters, the higher efficiency of the PV device will be.

The energy conversion efficiency of the photovoltaic solar cell depends on several diffierent external factors. Among these factors are:

- The conversion efficiency relies on the wavelength of the light. Therefore, the efficiency of the photovoltaic cell will change with the variations in the spectrum of the sunlight [35, 36].

- The conversion efficiency depends on the temperature. The photovoltaic module will depend on the temperature of the surrounding air [37,38] .
- The conversion efficiency of the module depends on the reflectivity of the solar cell, encapsulation material, and the glass which accommodates the cells. The effects depend in particular on the angle on which the incoming light hits the module's surface [39, 40].

By taking in account all of the mentioned effects above, the operational conversion efficiency of the photovoltaic modules results in a deviation from the conversion efficiency of the solar cell under Standard Test Condition (STC). STC defines the measurements conditions at temperature of 25 °C, 1000 W/m2 irradiance and AM1.5 Air Mass global spectrum [41].

5.5. The quantum efficiency (QE)

The quantum efficiency (QE) is the ratio of carriers collected by a solar cell to the number of photons of a given energy that impact the cell, and it can be expressed as a function of wavelength or energy.

QE is an indicator of how good a solar cell is at the conversion of light to electricity .

Two types of *QE* measurements for solar cells can be considered:

1) External Quantum Efficiency (EQE), which includes the effects of optical losses such as transmission through the cell or reflection of light.

2) Internal Quantum Efficiency (IQE), which considers only the portion of light that is able to generate carriers.

$$IQE = \frac{EQE}{1 - R - T} \qquad (1.9)$$

Where R and T are the reflection and transmission coefficient respectively.

IQE is a direct measurement of recombination and refers to solar cells ability to utilise photons.

In general, IQE is higher than EQE for a given device because the factor 1-R is always less than 1.

If the reflection and transmission of a device are known, the EQE curve can be calculated from the IQE curve.

Quantum efficiency in most solar cells is reduced due to recombination, impeding charge carriers to move to the external circuit. Also, any mechanism that affects the probability of collection of carriers also affects the QE. QE. as function of wavelength for different

materials used in solar cells are shown in figure 1.14. For wavelengths longer than the band gap, the QE is reduced to zero.

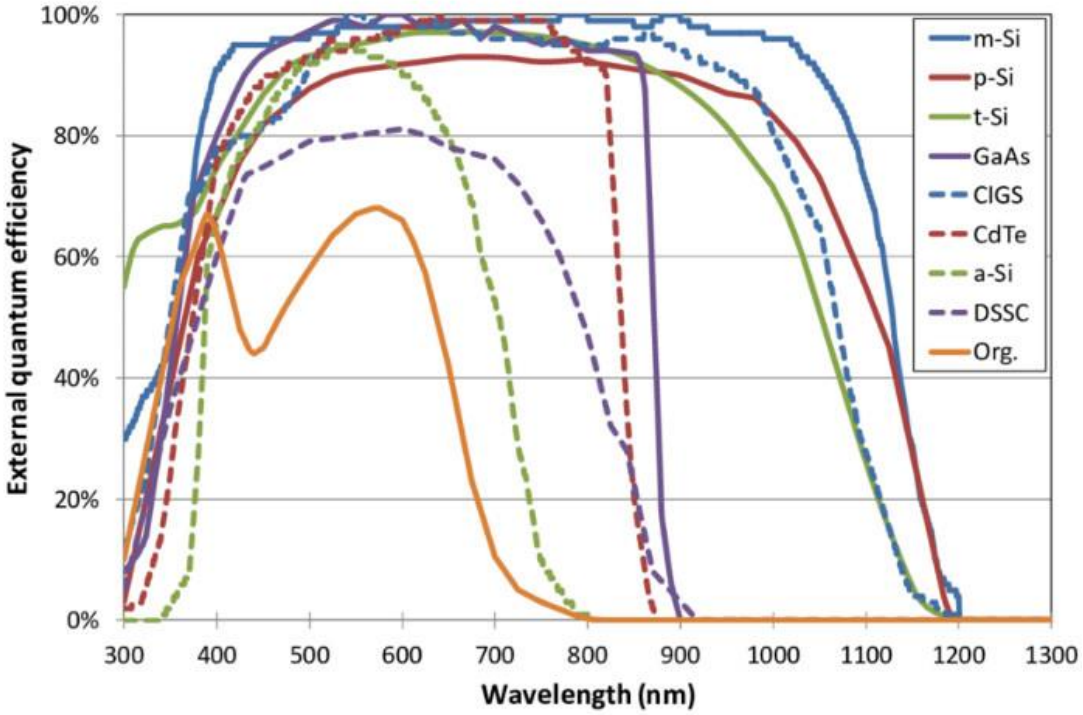

Figure 1.14: EQE graph for different materials used in solar cells[42].

5.6. Photo generated current

Although, the equation 1.4 is very helpful and can be solved for I_{SC} and V_{OC} by assuming I_{ph} is equal to the I_{sc}, it is not completely true for a real solar cell since the resistance of solar cell is neglected. A more general equation including the component of resistance needs to be included. Thus, Equation 1.4 can be extended as:

$$I = I_{ph} - I_0\left(e^{\left(\frac{q(V+IR_S)}{nkT}\right)} - 1\right) - \frac{V + IR_S}{R_{SH}} \qquad (1.10)$$

Here, R_S is the series resistance and R_{SH} is the shunt resistance of solar cell.

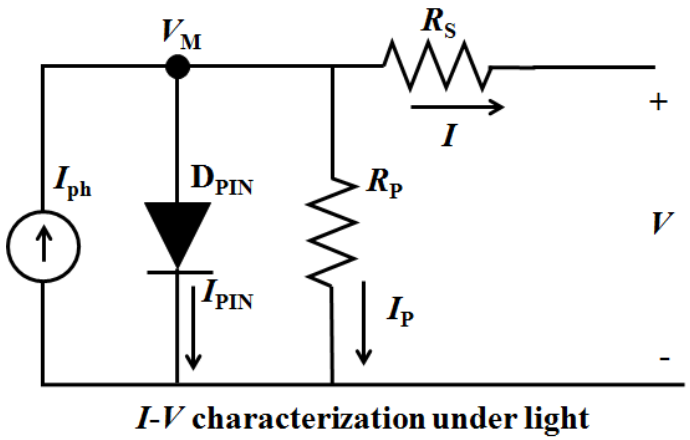

Figure 1.15: An equivalent circuit of a basic solar cell under illumination.

correlate the FF to R_S and R_{SH}. Ideally, an R_S as low as and an R_{SH} as high as possible is desirable for a solar cell. A schematic circuit equivalent of solar cell including R_S and R_{SH} is presented in figure 1.15. The effect of R_S and R_{SH} on solar cells FF is presented in figure 1.16. As can be seen I_{SC} and V_{OC} are not affected by R_S and R_{SH} unless R_S and R_{SH} are too high and too low, respectively.

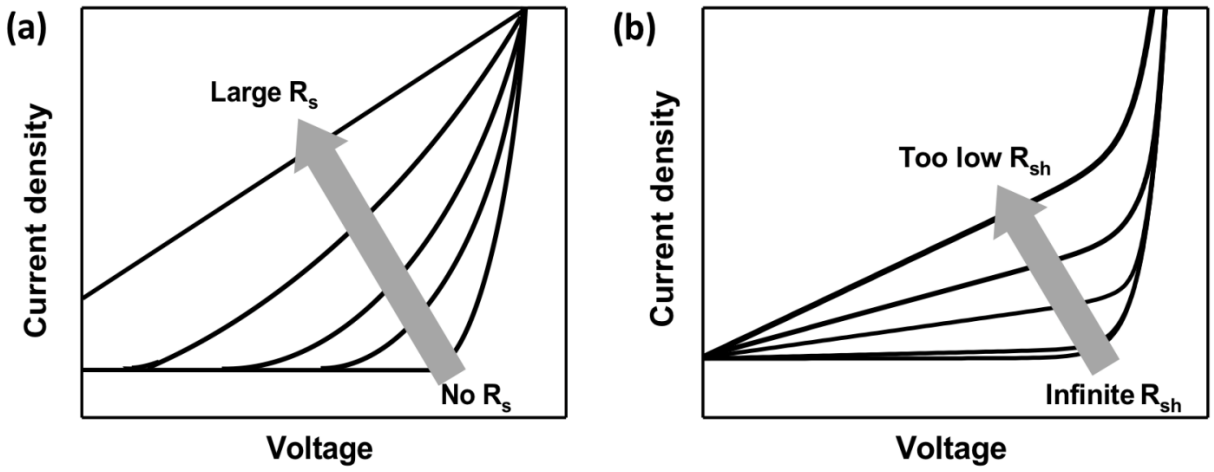

Figure 1.16: (a) *J-V* curve of solar cell as a function of R_S the direction of arrow indicates increasing R_S. (b) Evolution of the *J-V* curve with respect to R_{SH}, the direction of arrow shows the decreasing *Rsh*.

Chapter 2

Chapter 2 Material properties and application

1. Graphene

Graphene, a monolayer of sp2 bonded carbon atoms in a honeycomb lattice figure2.1 created a surge in research activities owing to its high current density, ballistic transport, chemical inertness, high thermal conductivity, optical transmittance, and super hydrophobicity at nanometer scale. Graphene is considered to be one of the miracle materials in the twenty-first century. The first report of employing a simple technique called micro mechanical cleavage to extract graphene has attracted worldwide attention and earned them the Nobel Prize in Physics in the year 2010. Though graphene was known well before that time, Geim and the group's research in 2004 created huge interest in the field.

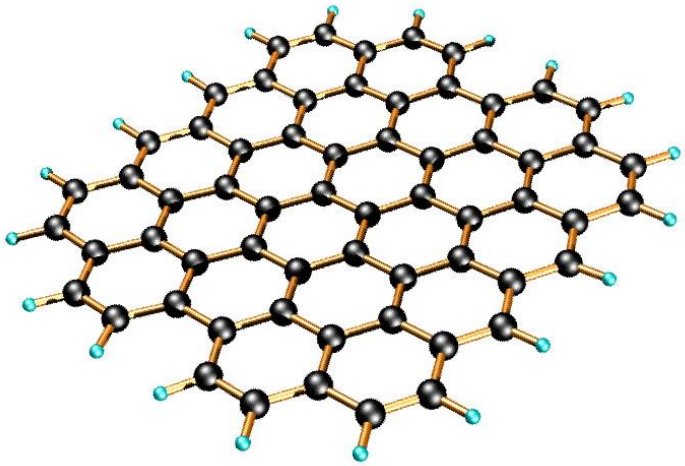

Figure 2.1: Graphene 2D Structure .

In a sense, graphene is more attractive than its allotrope, carbon nanotubes (CNTs) since the 2-dimensional form of graphene is much better, from the fabrication and application point of view, than 1-dimensional CNTs. Utilizing its extremely high mobility , stand-alone high frequency transistor with a cut-off frequency as high as 300 GHz could be designed. On the other hand, electromigration problems in interconnects could be avoided with high current capacity (108 A/cm^2) and low resistance (1 μΩ-cm: 35% less than Cu) of graphene. Graphene heat pad has shown good promise owing to its high thermal conductivity. Graphene can also be a strong candidate for replacement of ITO as a transparent electrode (which is a necessity as earth crust has very low reserve of Indium).

Graphene could have over 90% of transparency and 30 Ohm/square of sheet resistivity, making it most suitable for transparent conducting electrode applications.

Graphene has an extraordinary mechanical strength/weight ratio exceeding that of any known material. Graphene also has the highest surface to volume ratio, utilizing two-side surfaces. Thus, graphene-based chemical sensors can be used to detect explosives in luggage

and volatile organic compounds in air by converting chemical reactions into electrical signals. Graphene might revolutionize battery technologies, where it can be used as a super-conductive membrane between a battery's poles. This battery could supply a huge energy for a short period of time.

Graphene was originally visualized as a material that could replace Si in digital logic circuits since it exhibits excellent electrical properties, including very high electron mobility.

However, one problem is that graphene does not have a band gap, which is a necessary for a semiconductor. Furthermore, a graphene transistor is very difficult to turn off, with an on/off ratio as high as 1,000 at room temperature.

To open a stable band gap of ~1 eV, it is necessary to make graphene ribbons smaller than 2 nm wide with single atom precision. Variation in width of a graphene sheet results in deviation of band gap energy. Mobility of graphene is severely degraded if the ribbon edges are rough and if the substrate underneath is not flat. In turn, reproducibility issues are challenging for the success of future graphene nanoelectronics.

Graphene grown by the chemical vapor method is not a single crystal, due to unavoidable occurrence of nucleation and growth during the process. This leads to degradation and variation in properties of graphene-based electronic devices.

Graphene transistors have not yet revealed better analog properties over other single crystalline high mobility semiconductors (such as III-V compound semiconductor) since the transistors have already approached the range of almost 1 THz cut-off frequency. So, it seems that graphene's promise in next generation electronics is not easily achievable. Its future may lie elsewhere such as in passive devices and/or components less sensitive on variation of its energy band gap.

Silicon was discovered in 1824, but the first transistor was made by Bell Labs scientists in 1947. It took 123 years to create the first transistor, but with Ge. In contrast, CNT was discovered in 1991 and the first CNT transistor was demonstrated in 1998. Graphene was manufactured in the 2-D stable form through an easy and reproducible process in 2004 . Thus,we need some patience for the materialization of our dream in the application of nanocarbon materials—CNTs and graphene. Lots of research efforts should be made until some big breakthroughs happen with CNTs and graphene [43] .

Chapter 2 Material properties and application

2. Synthesis of graphene

Considerable efforts have been taken to make graphite samples that approach single-layer graphene.

Kim's group developed a method by attaching a graphite microcrystal to a tipless cantilever of atomic force microscope (AFM) and then scratched the crystal on silicon ubstrates [44] . Islands of graphite as thin as 10 nm, or ~30 layers were stamped on SiO2, figure 2.2.

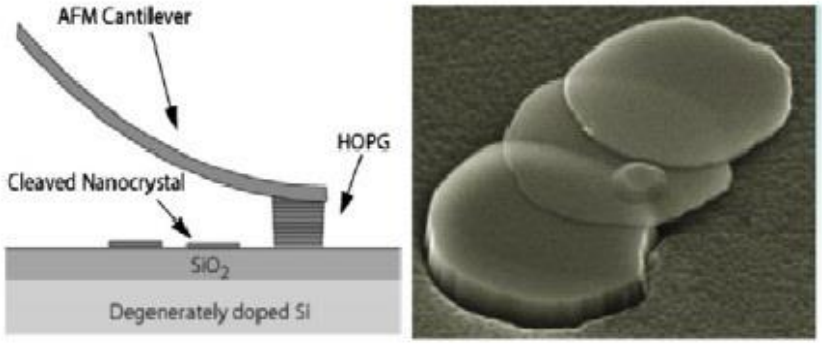

Figure 2.2: (Left) Schematic illustration of rubbing graphitic pancakes to substrates by AFM cantilever. (Right) Typical SEM image of graphitic pancakes received [45].

Even with this elegant method, the resulting material is still graphite, rather than graphene which is a single layer of graphite. The imaginary graphene was first made by Geim's group in University of Manchester in 2004 by mechanical cleavage of graphite[46]. Although this method is competent in giving high quality graphene with good electrical and optical properties satisfactory for most fundamental studies, it is tedious and unreliable because of its low yield. This method, therefore, hinders graphene from the realization of real applications.

To avoid these shortcomings, a few methods have been developed 1-Chemical vapor deposition (CVD) of carbon on Ni and Cu with hydrocarbon flow has realized wafer-scale production of few-layer and single-layer grapheme. However, the graphene obtained by this method has many defects and is non-uniform compared to that produced by micromechanical cleavage method. In addition, the need to transfer the as grown graphene to other substrates is also problematic. Last, the quantity produced by this method is far less than needed in other applications, such as scaffolds for tissue engineering [47] .

2-. To fully investigate the electrical properties, efforts are made on the epitaxial growth of graphene film to generate high-quality graphene and considerable progress has been achieved.

However, it should be noted that this method relies heavily on expensive silicon carbide substrates and strict conditions, e.g. UHV vacuum. Therefore, this method is of limited value for practical applications.[48] .

3-. More recently, liquid phase exfoliation of graphite appears to be a simpler and cheaper method to make graphene. However its low yield (~1wt %) and small pieces of graphene obtained prove disadvantageous.

Table 2.1 lists several common techniques to obtain graphene-based materials. The chemical exfoliation method[49]. is the most flexible, low cost and simplest.. While the electrical properties of graphene oxide (GO, referred to as the single layer of graphite oxide, similar to graphene that is single layer of graphite.) is not preserved, other characteristics and properties are worth investigation and may make graphene oxide useful for a range of applications, e.g. as a component of composite materials. Reduced graphene oxide (rGO) could be obtained by reduction of graphene oxide, enabling it to be used like graphene, as reported by several papers. The process for obtaining rGO potentially opens up many applications. For example, rGO has been used as substrates for field emitters,charge carriers, or transparent electrodes for solar cells [50] .

Method	Advantages	Problems
MMC[a]	– Pristine and perfect graphene with few defects – Useful for fundamental research	– Low throughput and unreliable
CVD[b]	– Inexpensive (Ni, Cu) – Wafer-scale	– Non-uniform – High temperature – Low yield of single-layer
EG[c]	– Relatively large pieces for device fabrication	– Too expensive of the growth substrates (SiC) – - Strict conditions required, e.g. UHV
LPE[d]	– Facile way to make nearly-perfect graphene	– Low yield – Piece too small to integrate with fabrication
CE[e]	– Large yield – Cheap and affordable – High solubility in solvents and transferrable to various substrates	– Deteriorated electrical properties (graphene oxide, not graphene)

[a]Micromechanical cleavage method ("scotch tape method")
[b]Chemical vapor deposition method
[c]Epitaxial growth method
[d]Liquid phase exfoliation method
[e]Chemical exfoliation method

Table 2.1: Comparison of various methods to produce graphene[49].

3. Graphene properties

3.1. Conductivity and Mobility

pristine graphene is a zero-band gap semiconductor with extraordinary room temperature carrier mobility 200,000 cm^2/Vs at RT in comparison with 1,400 cm^2/Vs for Si and 8500 cm^2/Vs for GaAs, but to understand this from a chemist's point of view, it is helpful to start with a structural perspective. Each carbon atom in graphene's hexagonal lattice has four valence electrons; the first three are used to form covalent sp2 bonds, while the fourth resides in a pz orbital that forms π bonds distributed equally along 3 directions thus leading to a bond order of 1 and 1/3. Hence, a continuous layer of delocalized electrons forms across each plane that enables the rapid movement of injected electrons figure 2.3(a-b).

Physicists generally explain this remarkable conductivity as a consequence of a zero band

gap,which can be mathematically derived by first assuming that graphene has two identical carbon atoms per unit cell figures 2.3(c-d) [51] .

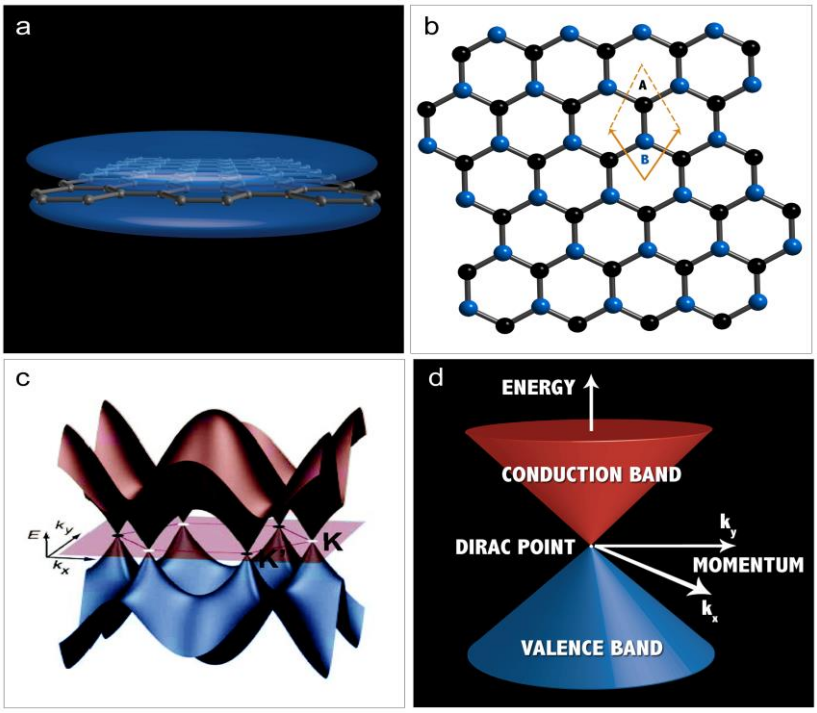

Figure 2.3: (a-b) Graphene's band structure (c-d). a zero-band gap at the Dirac point [51]

3.2. Thermal Properties

In addition to being electronically conductive, graphene also exhibits a phenomenally high thermal conductivity and this observation is a consequence of its atomic structure. While graphene's sp2 hybridized system allows for the ballistic transport of electrons, its rigid covalent bonds are responsible for the quick dissipation of lattice vibrations known as phonons, which leads to extremely high thermal conductivities (κ) = 3-5 $kW.mK^{-1}$ 10 times larger than Cu and Al at room temperature [52].

The thermal properties of materials are known to change when the dimensions are reduced to the nanometer scale[53]. Heat conduction in lower dimensions is predicted to have an infinitely large intrinsic κ, because transport is confined to just one lateral dimension.

3.3. Optical Properties

Graphene shows remarkable optical properties. An example is that it can be visualized on silicon dioxide as it forms an interference pattern, even though it is only one atomic layer thick [54] .

Figure 2.4 (a) shows CVD grown graphene transferred onto a silicon/silicon dioxide substrate.

Chapter 2 Material properties and application

Graphene's transmittance can be expressed in terms of a fine-structure constant and can be derived using principles for thin-films with a fixed universal optical conductance [55] .

The transparency of a single layer of graphene in the visible region has been both calculated and measured to be ~97.7% figure 2.4 (b-c).

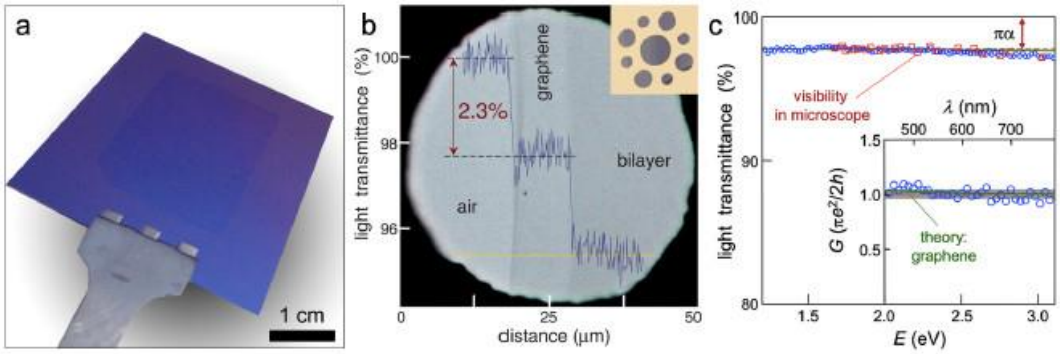

Figure 2.4: Graphene optical properties [55] .

3.4. Mechanical propreties of graphene

Graphene received the title of "strongest material ever" after the confirmation of its sustaining breaking strengths of 42 N/m with an intrinsic mechanical strain of ~ 25% and Young's modulus of Y ~ 1.0 TPa . Its mechanical thickness can also be controlled as demonstrated through mechanical stress measurements performed on graphene sheets subjected to deformations induced by depositing different insulating capping layers .

The experimental findings regarding the main mechanical features of graphene have been confirmed by several theoretical works using different techniques

3.5. High Surface Area

The surface area of nanomaterials is generally very high and graphene, with a calculated value of 2630 m2 g^{-1}, is no exception [56] .

In general, high surface area translates into increased reactivity. Since graphene comes in several varieties, these should be considered separately.

The largest concern for pristine graphene is that up to half of the area is impeded by its interactions with a support structure. Due to a lack of high-throughput methods, there is no practical way so far to obtain large quantities of suspended graphene, so typically only one side is exposed.

Graphene's high surface area may also find use in improving battery electrodes, especially since carbon is an earth abundant material [57] .

Chapter 2 Material properties and application

4. Graphene application

The interest in graphene has mobilized both academic and industry realms making it an ideal candidate for the design of modern nanoscale transistors, chemical and biosensors, flexible and organic light-emitting diodes (OLEDs) displays, solar and fuel cells, and other innovations. The restricted graphene mass-production and limited reproducibility in device performances are still important matters that researchers should consider in order to push graphene-based technology into a commercial status.

However, the fast development of graphene research leaves no doubt that this material will revolutionize several markets such as electronics, medicine, and energy storing in the near future.

Medicine studies can also benefit from graphene"s amazing properties. In particular, graphene possesses great sensorial response to external analytes, enabling the design of nanosensors to diagnose diseases . Accurate biosensors can be created from DNA-functionalized graphene samples, which are capable of detecting external DNA genes associated with diseases .

Graphene can also have a huge impact in environmental monitoring applications bolstered by the design of graphene-based nanoscale gas sensors .

Another attractive innovation based on graphene materials reaches the electronics scope where researchers have been able to develop bendable transparent and conductive membranes composed of graphene for engineering flexible-panel displays.

Recent studies have revealed that graphene-based OLEDs can even top the performance of indium tin oxide (ITO) compounds, commonly used in transparent conductive electrodes. Graphene is also considered to be the basis of future computing chips after the successful realization of high-speed graphene-based transistors operating at outstanding cutoff frequencies of 700–1400 GHz .

All these important innovations, which were generated after the first isolation of graphene layers, indicate that the use of these materials is not limited to providing simply a theoretical model that can describe the physical properties of several organic nanostructures. Graphene is occupying a centerpiece position in many scientific advances that can change our way of making and using technology. As mentioned by A.K. Geim, we are witnessing a scientific excitement similar to the one experienced around 100 years ago with the discovery of polymers that recently supplied our lives with plastics. We expect that the innovations resulting from graphene will prove even more exciting [43] .

Chapter 2 Material properties and application

5. Graphene oxide

Graphene oxide(GO) is a two dimensional material derived from graphite oxide which is a compound of carbon, oxygen and hydrogen in variable ratios figure2.5.

It was first prepared by Oxford chemist Benjamin C Brodie in 1859 and developed by Hummers and Offeman in 1957 [58]. Recently graphene oxide has drawn intensive research interests because its role of being a precursor of graphene by reduction.

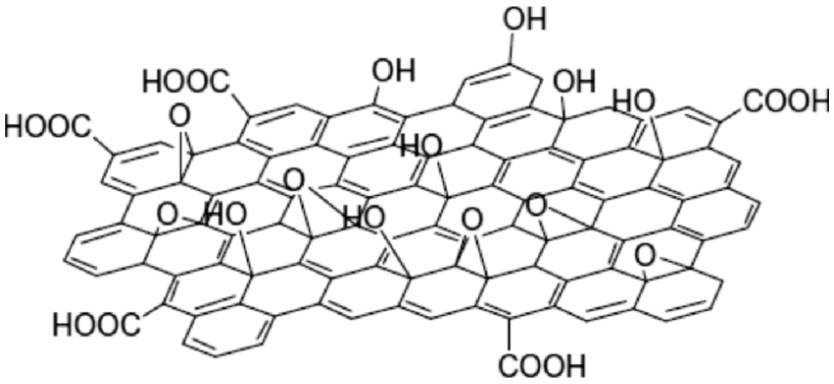

Figure2.5: Graphene oxide 2D Structure

Graphite oxide has a similar layered structure to graphite but the plane of carbon atoms in graphite oxide is heavily decorated by oxygen-containing groups, including carbonyl (C=O), hydroxyl (-OH), epoxy (C-O-C) and carboxyl (COOH) groups .

Thus, these layers can be exfoliated in water under moderate ultra-sonication resulting in thin films of graphene oxide. These films can be partially reduced by removing the oxygen containing groups through chemical, sonolytic, microwave, photo thermal, photo catalytic and electrochemical methods [59].

6. Graphene oxide reduction

Graphene oxide can be solely reduced by heat treatment which is called thermal annealing reduction. Rapid heating (>2000OC/min) was usually used to exfoliate graphite oxide to achieve graphene due to the sudden expansion of CO or CO2 gases evolved into the spaces between sheets during the rapid heat The rapid temperature increase also makes the oxygen-containing functional groups attached to carbon atoms decompose into gases figure 2.6 [60].

Chapter 2 Material properties and application

Figure 2.6 : Diagram of reduced graphene oxide (rGO)

7. Silicon

Silicon is obtained from quartzite reduction with carbon in an arc furnace .

The product of this process is called metallurgic grade silicon which has about 98% Purity . This material is not pure enough for microelectronics fabrication so a process of refraction is due to improve quality. The milled metallurgic silicon is exposed to hydrochloric gas in a fluidized-bed reactor. The reaction is given by $Si+3HCl \rightarrow SiHCl_3+H2$, where the hydrogen is taken away at temperatures below of 30 °C at which the trichlorosilane is liquid.

The trichlorosilane is used and the chlorides are separated using distillation columns, at the end of the process the silicon is highly pure [61] .

Defects in silicon have an influence in the performance of the devices. Some defects are vital but others fatal. For the semiconductor industry controlled substitution is essential for a good performance however a high addition of elements let the material useless. the defect gives different properties to the material affecting the functioning of the device. The grade of perfection of the silicon and amount of impurities affect the lifetime of minority charge carrier although structural defects can operate as recombination spots [62].

There are different alternatives for solar cells when the material selected is silicon. Depending on the fabrication process the silicon ingot can grow crystalline or amorphous and each one has different characteristics and advantages that make them suitable for this application.

7.1. Monocrystalline Silicon

Crystalline materials can grow either monocrystalline or polycrystalline according to the technique implemented. Monocrystalline silicon are created using methods such as Czochralski, Float-Zone and Ribbon-Growth. The most common method to grow monocrystalline silicon is the Czochralski (CZ) method. This technique consists in melting

pure polycrystalline silicon in a quartz crucible and pull up a monocrystalline seed at controlled temperature, rotation speed and pull-up speed. The seed has the required crystal orientation. A small amount of p-type doping material can be added to the molten silicon to create p-doped silicon [63].

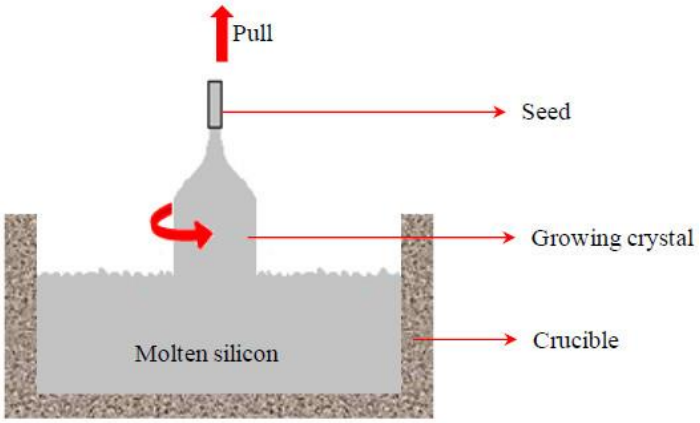

Figure 2.7 : Schematic of Czochralski growth [63].

7.2. Polycrystalline Silicon

The production of polycrystalline silicon is easier than the monocrystalline version reducing the costs of manufacturing but also the efficiency. One of the main advantages is the fact that it is no necessary an extra cutting step of the sides because of the square/rectangular shape that can be achieved. The most used methods for obtaining multicrystalline silicon are block-casting, Bridgman process and ribbon growth [64].

The most common method to grow polycrystalline silicon is The Ribbon-growth technique is a group of methods created to avoid the necessity for slice the ingot to get the wafer.

It consists basically of the continuous production of a thin sheet from the melted silicon diverse techniques are used to establish the edges of the ribbons [63].

They were created at research and development projects in different companies and in this moment just few of them are used in mass production and the most known are edge-defined film edge growth (EFG), string ribbon (SR) and dendritic web technology (WEB).

EFG and SR produce large grain ribbons [64].

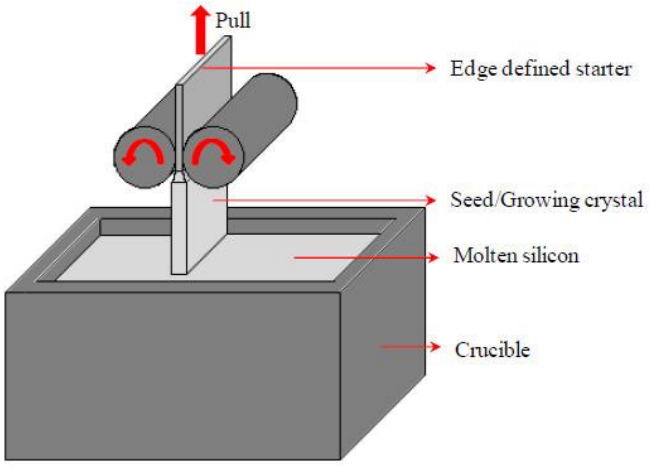

Figure 2.8 : Schematic of film edge growth EFG [64].

7.3. Amorphous Silicon

Amorphous silicon is fabricated by deposition of silicon in presence of silane (SiH4) gas using 'glow discharges' (plasma deposition) or evaporation .The electrical properties are fairly good but better for plasma deposited amorphous silicon.

These properties can be improved by doping the thin film by mixing the silane with diborane (B2H6) or phosphine (PH3) gas creating p-doped and n-doped amorphous silicon.

Research has been done to improve properties of amorphous silicon. Optoelectric properties, for example, has been enhanced by bonding hydrogen to the plasma deposited silicon . This new structure is called hydrogenated amorphous silicon (a-Si:H). The amorphous silicon is attractive due to its relatively low cost and simple, as well as its capability to be used as solar cell but the efficiency is still low (<10%) compared to the crystalline versions [65].

8. Propreties of silicon

Silicon is semiconductor with a bandgap of 1.12 eV, which means that pure silicon at room temperature is almost an insulator. By doping with group III or group V elements, the resistivity of silicon can be varied over a wide range Also Silicon is a hard, brittle material, and at room temperature under stress silicon single crystal elongates elastically until fracture stress appears without significant plastic deformation Although silicon is opaque in the visible range of the optical spectrum, it is transparent in the near infrared. It is highly reflective and has a large index of refraction The previous silicon properties can be summarized in the table 2.2 .

Chapter 2 Material properties and application

Atomic number of Si	14	
Atomic mass of Si	28 (92.23%)	29 (4.67%), 30 (3.1%)
Crystal structure	Diamond	
Lattice constant	0.5431	nm
Si atoms	$5x10^{22}$	atoms*cm^{-3}
Melting point	1687	K
Specific density	2.329	g*cm^{-3} at 298 K
Specific density (liquid)	2.57	g*cm^{-3}
Thermal conductivity	149	W*$m^{-1}K^{-1}$
Coefficient of thermal expansion	$2.56x10^{-6}$	$m^{-1}K^{-1}$ (at 298 K)
Specific heat capacity	19.79	J*$mol^{-1}K^{-1}$
	0.705	J*$g^{-1}K^{-1}$
Young's modulus	150	GPa
Speed of sound	8433	m*s^{-1}
Hardness	7	Mohs
Hardness	850	kg*mm^{-2} (Knoop hardness)
Volumetric compression coefficient	$1.02x10^{-8}$	kPa^{-1}
Index of refraction (varies with temperature and λ)	~3.54 ~3.48	λ 1.1 μm, RT λ 2 μm, RT

Table 2.2: basic parameters of silicon [66].

Chapter 3

Chapter 3 Results and discussion

1. Silvaco ATLAS simulation software

Silvaco's ATLAS software offers general capabilities for two and three-dimensional simulation of semiconductor devices. ATLAS is used via DeckBuild, an interactive runtime environment. Figures can be made from the data obtained from the simulation and plotted using TONYPLOT, the included interactive graphics and analysis package. ATLAS has a comprehensive collection of physical models that are of use for modeling solar cells .

The ATLAS defined solar cell structure and composition requires several parameters to be defined. These basic parameters include a two-dimensional, fine division of the overall material called a mesh, the division of that mesh into regions, the assignment of materials to each region. Next, the electrode locations must be defined. Then, doping must be introduced into the respective materials. Also, a specification of a light spectrum for simulation must be made. The next step for the user is to choose among different models, finding that which is most the suitable for evaluating the structure, and achieving a better outline for the specific cell simulation.

2. Features and Capabilities of ATLAS

ATLAS provides a comprehensive set of physical models, including:

• DC, AC small-signal, and full time-dependency.
• Drift-diffusion transport models.
• Energy balance and Hydrodynamic transport models.
• Lattice heating and heatsinks.
• Graded and abrupt heterojunctions.
• Optoelectronic interactions with general ray tracing.
• Amorphous and polycrystalline materials.
• General circuit environments.
• Stimulated emission and radiation
• Fermi-Dirac and Boltzmann statistics.
• Advanced mobility models.
• Heavy doping effects.
• Full acceptor and donor trap dynamics
• Ohmic, Schottky, and insulating contacts.
• SRH, radiative, Auger, and surface recombination.
• Impact ionization (local and non-local).

Chapter 3 Results and discussion

• Floating gates.

• Band-to-band and Fowler-Nordheim tunneling.

• Hot carrier injection.

• Quantum transport models

• Thermionic emission currents.ATLAS

3. ATLAS inputs and outputs

Figure 3.1 shows the types of information that flow in and out of ATLAS. Most ATLAS simulations use two input files. The first input file is a text file that contains commands for ATLAS to execute. The second input file is a structure file that defines the structure that will be simulated, Therefore ATLAS produces three types of output files. The first type of output file is the run-time output, which gives the progress and the error and warning messages as the simulation proceeds. The second type of output file is the log file, which stores all terminal voltages and currents from

the device analysis. The third type of output file is the solution file, which stores 2D and 3D data relating to the values of solution variables within the device at a given bias point.

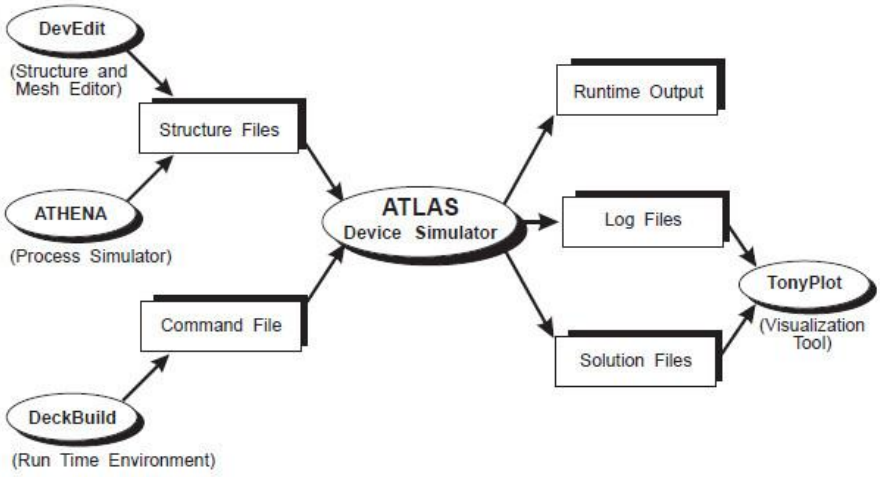

Figure 3.1: ATLAS Inputs and Outputs [67]

4. Statements and parameters

The input file contains a sequence of statements. Each statement consists of a keyword that identifies the statement and a set of parameters. The general format is:

<STATEMENT> <PARAMETER>=<VALUE>

For any <STATEMENT>, may have four different types for the <VALUE> parameter. These are: Real, Integer, Character, and Logical.

An example of a statement line is:

DOPING UNIFORM REGION=4 N.TYPE CONCENTRATION=1e15

The statement keyword must come first but after this, the order of parameters within a statement is not important.

5. Running ATLAS inside Deckbuild

Each ATLAS run inside DECKBUILD should start with the line:

GO ATLAS

A single input file may contain several ATLAS runs each separated with a GO atlas line. Input files within DECKBUILD may also contain runs from other programs such as ATHENA or DEVEDIT along with the ATLAS runs.

6. Structure simulation using ATLAS

The order in which statements occur in an ATLAS input file is important. There are five groups of statements that must occur in the correct order, figure 3.2. Otherwise an error message to appear, which may cause incorrect operation or termination of the program. For example, if the material parameters or models are set in the wrong order, then they may not be used in the calculations.

Group	*Statements*
1. Structure Specification	MESH REGION ELECTRODE DOPING
2. Material Models Specification	MATERIAL MODELS CONTACT INTERFACE
3. Numerical Method Selection	METHOD
4. Solution Specification	LOG SOLVE LOAD SAVE
5. Results Analysis	EXTRACT TONYPLOT

Figure 3.2: ATLAS Command Groups with the Primary Statements in each Group

6.1. Structure Specification

The structure specification is done by defining the mesh, the region, the electrodes and the doping levels

In this Study we choose a similar structure from a real device experiment figure 3.3 [68]

Chapter 3 Results and discussion

It consists of 100 μm n.type single c-Si wafer (doping density: $1 \times 10^{15}\ cm^{-3}$) with 10 nm of graphene layer depositing on the Si surface and 200 nm of silver (Anode) Where formed on the graphene film to prepare a square windows $\approx$ 0.09 cm^2 to be close enough to the real structure as shown in Figure 3.4 .

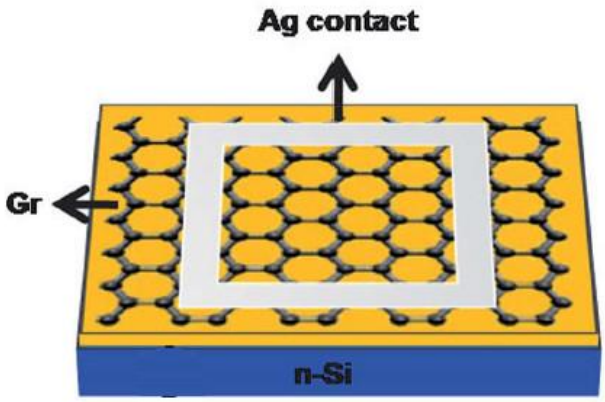

Figure 3.3 : Experimental solar cell structure

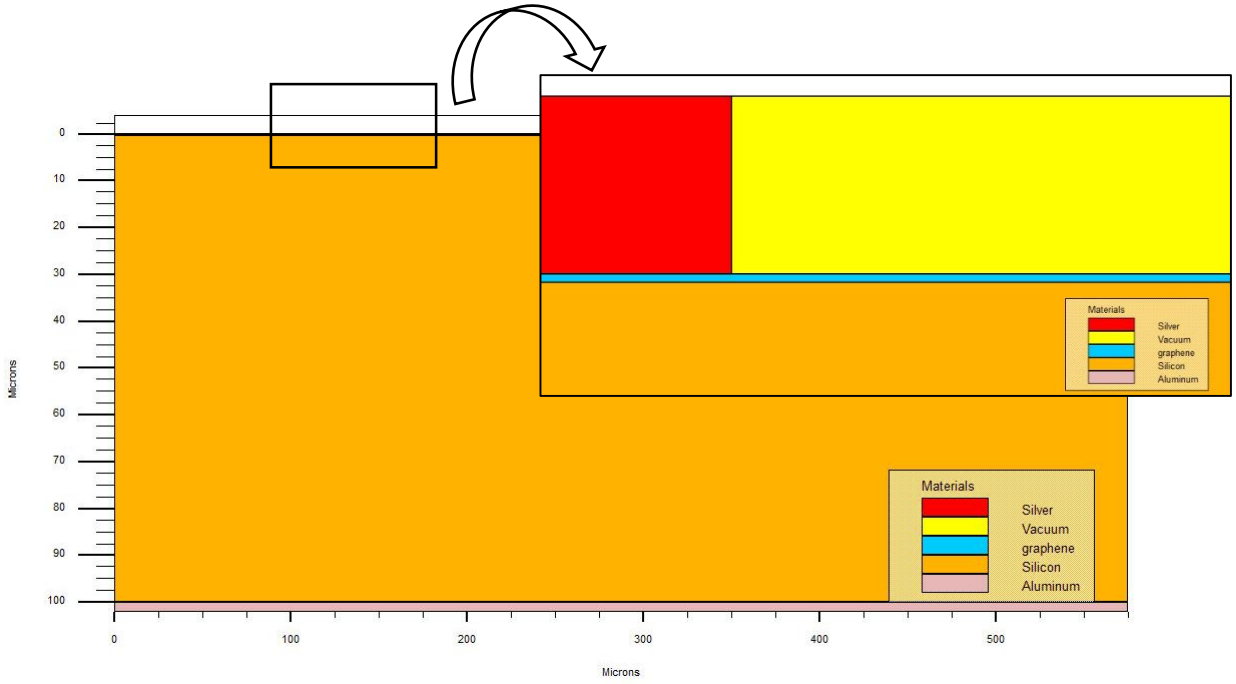

Figure 3.4 : structure using ATLAS

6.1.1. Specifying Mesh

The first section of structure defining statements in the Deckbuild program is the meshing section. this section specifies the two dimensional grid that is applied to the device with mesh statements.

The following instruction is used to define the meshing:

MESH SPACE.MULT=<VALUE>

X.MESH LOCATION=<VALUE> SPACING=<VALUE>

Y.MESH LOCATION=<VALUE> SPACING=<VALUE>

Mesh statements have two parts called location statements and spacing statements.

The location statement "loc" specifies the x or y value in the structure to which the following "spacing" statement is applied while, the spacing statement "space" specifies the spacing between grid lines at that specific location.

The ATLAS device simulator can more easily solve the differential equations at each grid point if there are no abrupt changes between adjacent points. Therefore the structure must has a very adequate mesh density especially in the critical areas like the interface between Si and graphene (depletion region) or graphene and silver (contact) as shown in figure 3.5

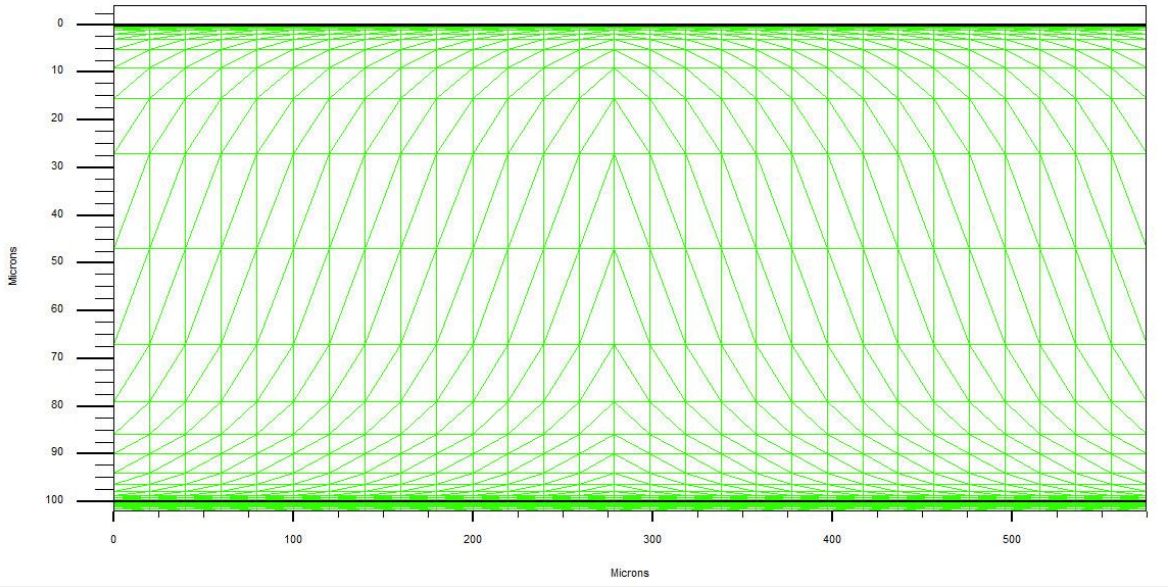

Figure 3.5: ATLAS mesh

6.1.2. Specifying Regions

Once the mesh is specified, every part of it must be assigned a material type. This is done with REGION statements. For example:

REGION number=<integer> <material_type> <position parameters>

Region numbers must start from 1 to 200 as maximum number of regions in ATLAS.A large number of materials is available. If a composition-dependent material type is defined, the x and y composition fractions can also be specified in the REGION statement.

The position parameters are specified in microns using the X.MIN, X.MAX, Y.MIN, and Y.MAX parameters. If the position parameters of a new statement overlap those of a

previous REGION statement, the overlapped area is assigned as the material type of the new region.

All mesh points in the structure must be assigned to material. If this isn't done, error messages will appear and ATLAS won't run successfully.

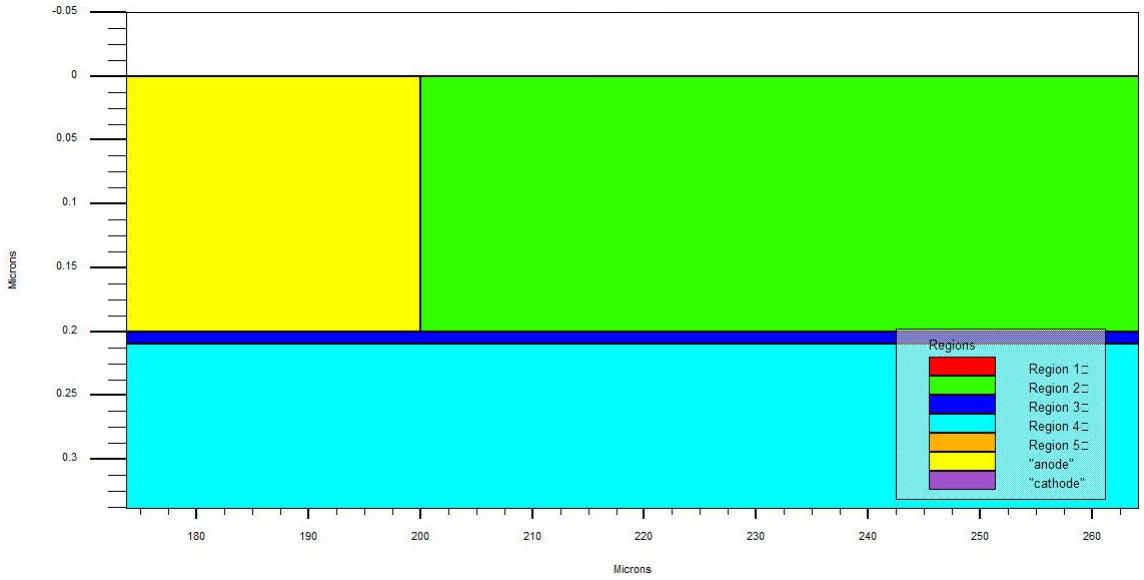

Figure 3.6: ATLAS regions with materials defined.

6.1.3. Specifying Electrodes

Once the regions and materials are specified, one electrode at least must be difined that contacts a semiconductor material. This is done with the ELECTRODE statement.For example:

ELECTRODE NAME=<electrode name> <position_parameters>

Up to 50 electrodes can be specified The position parameters are specified in microns using the X.MIN, X.MAX, Y.MIN, and Y.MAX parameters. Multiple electrode statements may have the same electrode name. Nodes that are associated with the same electrode name are treated as being electrically connected.

Some shortcuts can be used when defining the location of an electrode. If no "y" coordinate parameters are specified, the electrode is assumed to be located on the top of the structure. the RIGHT, LEFT, TOP, and BOTTOM parameters also can use to define the location.

Chapter 3 Results and discussion

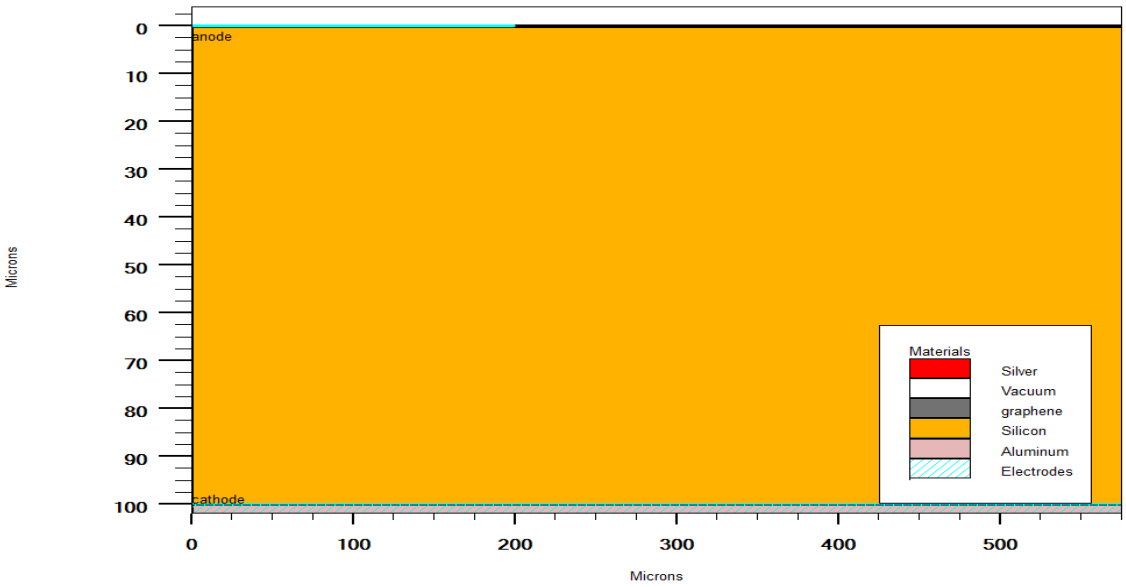

Figure 3.7: Atlas electrodes.

6.1.4. Specifying Doping

The doping could be specified using the DOPING statement. For example:

DOPING <distribution_type> <dopant_type> <position_parameters>

The simulated structure in this work has only one region (silicon) doped of n-type with concentration of 10^{15} cm^{-3} as shown in figure 3.8.

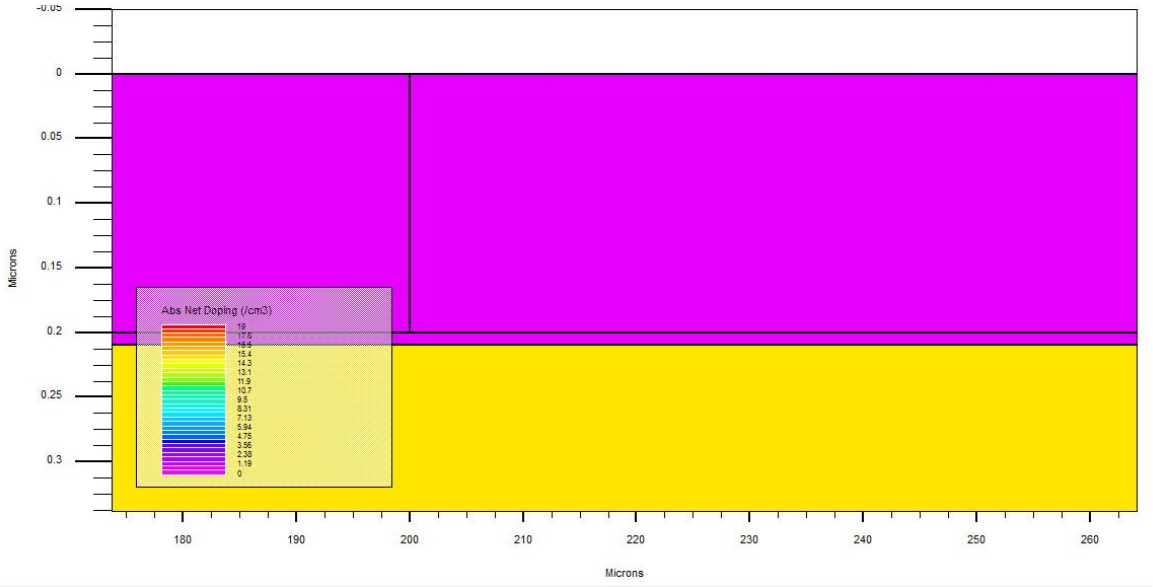

Figure 3.8: The doping distribution in regions

6.2. Defining Material Parameters and Models

Once the mesh, geometry, and doping profiles are defined, the characteristics of electrodes, and the default material parameters could be changed , and choose which physical models

Chapter 3 Results and discussion

ATLAS will use during the device simulation. These actions are accomplished using the CONTACT, MATERIAL, and MODELS statements respectively.

6.2.1. Specifying Contact Characteristics

An electrode in contact with semiconductor material is assumed by default to be ohmic. If a work function is defined, the electrode is treated as a Schottky contact. The CONTACT statement is used to specify the metal workfunction of one or more electrodes. The NAME parameter is used to identify which electrode will have its properties modified.
The WORKFUNCTION parameter sets the workfunction of the electrode. For example, the statement:

CONTACT NAME=anode WORKFUNCTION=5.1

6.2.2. Specifying Material Properties

The MATERIAL statement allows to specify the values for the basic parameters.
the values can apply to a specified material or a specified region. For example :

MATERIAL MATERIAL=Silicon EG300=1.12 MUN=1100

This statement sets the band gap and low field electron mobility in all silicon regions in the device. If the material properties are defined by region, the region is specified using the REGION or NAME parameters in the MATERIAL statement. For example, the statement:

MATERIAL REGION=2 TAUN0=2e-7 TAUP0=1e-5

A specific example of graphene used in this thesis is presented in table 3.1 [69]

identifier	EG300	MUN	MUP	NC300	NV300	affinity	Permittivity
value	0.026	16983.69	16983 .69	1.9e16	1.9e16	5	6

Table 3.1: graphene parameters used in simulation

6.2.3. Specifying Physical Models

To get the simulation to the realistic level, a lot of complex dependencies of the device properties must be taken in consideration such as the mobility variation as a function of carriers' concentration. These complexities are not necessary in some cases, so to avoid the

additional calculations, ATALS provides independent models to describe every device property dependence alone, so they can be activated separately. The accuracy of the results obtained depends on the models used in the simulation process.

The physical models fall into five categories: mobility, recombination, carrier statistics, impact ionization, and tunneling. The syntax of the model statement is as follows:

MODELS <model-name>

For example, the statement:

MODELS CONMOB FLDMOB SRH FERMIDIRAC

Note: The PRINT parameter lists to the run time output the models and parameters, which will be used during the simulation. This allows to verify models and material parameters.

For example we used in our study the bipolar model which Selects a default set of models as : CONMOB (Concentration Dependent), FLDMOB (Parallel Electric Field Dependence), BGN (Bandgap Narrowing), CONSRH (Concentration dependent lifetime Shockley Read Hall), and AUGER .

6.3. Numerical METHOD selection

Several different numerical methods can be used for calculating the solutions to semiconductor device problems. Numerical methods are given in the METHOD statements of the input file.

Different combinations of models will require ATLAS to solve up to six equations. For each of the model types there are basically three types of solution techniques: (a) decoupled (GUMMEL), (b) fully coupled (NEWTON) and (c) BLOCK. The GUMMEL method will solve for each unknown in turn keeping the other variables constant, repeating the process until a stable solution is achieved. The NEWTON method solve the total system of unknowns together.

The BLOCK methods will solve some equations fully coupled, while others are de-coupled. Generally, the GUMMEL method is useful where the system of equations is weakly coupled, but has only linear convergence. The NEWTON method is useful when the system of equations is strongly coupled and has quadratic convergence. The NEWTON method may however spend extra time solving for quantities which are essentially constant or weakly coupled. NEWTON also requires a more accurate initial guess to the problem to obtain convergence. Thus, a BLOCK method can provide for faster simulations times in these cases over NEWTON.

Chapter 3 Results and discussion

GUMMEL can often provide better initial guesses to problems. It can be useful to start a solution with a few GUMMEL iterations to generate a better guess and then switch to NEWTON to complete the solution. Specification of the solution method is carried out as follows:

METHOD GUMMEL BLOCK NEWTON

6.4. Obtaining Solutions

ATLAS can calculate DC, AC small signal, and transient solutions. Obtaining solutions is rather analogous to setting up parametric test equipment for device tests. by define the voltages on each of the electrodes in the device. ATLAS then calculates the current through each electrode. ATLAS also calculates internal quantities, such as carrier concentrations and electric fields throughout the device. This is information that is difficult or impossible to measure.

In all simulations, the device starts with zero bias on all electrodes. Solutions are obtained by stepping the biases on electrodes from this initial equilibrium condition.

NOTE: When no previous solutions exist, the initial guess for potential and carrier concentrations must be made from the doping profile. This is why the initial solution performed must be the zero bias (or thermal equilibrium) case. This is specified by the statement:

SOLVE INIT

6.5. Interpreting Results

Simulation produces three different types of output files :

1-If the PRINT option specifed within the MODELS statement, the details of material parameters and constants and mobility models will be specified at the start of the run-time output. This is a useful way of checking what parameters values and models are being applied in the simulation.

2-Log files store the terminal characteristics calculated by ATLAS. These are current and voltages for each electrode in DC simulations. In transient simulations, the time is stored. In AC simulations, the small signal frequency and the conductances and capacitances are saved. For example, the statement:

LOG OUTF=<FILENAME>

Chapter 3 Results and discussion

3-The EXTRACT command is provided within the DECKBUILD environment. It allows to extract device parameters. The command has a flexible syntax that allows to construct specific EXTRACT routines. EXTRACT operates on the previous solved curve or structure file. By default, EXTRACT uses the currently open log file. To override this default, supply the name of a file to be used by EXTRACT before the extraction routine. For example:

EXTRACT INIT INF="<filename>"

Note: Over 300 examples are supplied with ATLAS to provide many practical examples of the use of the EXTRACT statement [67].

7. Simulation results and discussions

7.1. The graphene/silicon solar cell simulation

Our study is based on real experiment, we have simulated the closest structure to the real graphene/silicon solar cell and we took into account all sides (the same dimension, material and the same conditions of experiment), we get with SILVACO ATLAS the J-V curve figure 3.9, and we compared the experimental and the simulated results as shown in table 3.2.

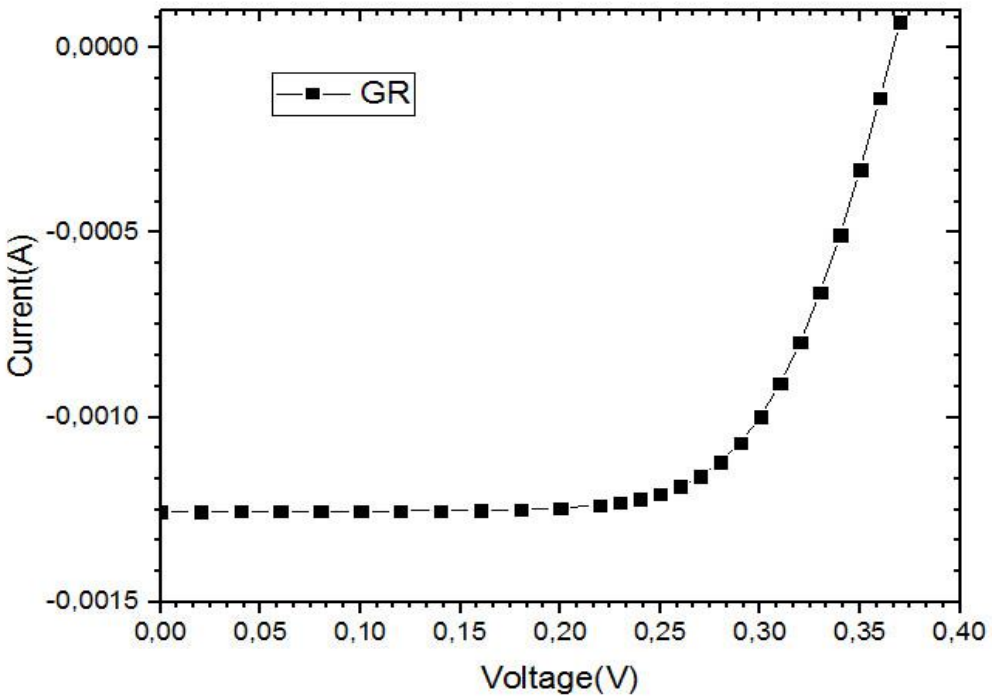

Figure 3.9: Graphene/Silicon J-V characteristic using ATLAS

Chapter 3 Results and discussion

Results	$Jsc(mA.cm^{-2})$	$Voc(V)$	$FF(\%)$	$Eff(\%)$
Our results	8.78	0.36	68.18	2.27
Experimental results	6.5	0.42	56	1.7

Table 3.2 : Comparison between parameters of the solar cell [68]

The results between the experimental and simulation are almost close, the difference may be due to some imperfections such as:

-3D simulation may have better result.

-Difference between Parameters of material used in experiment and what we find in our research.

7.2. Effect of graphene thickness on solar cells

In this section we will study the effect of the graphene layer thickness on the J-V characteristic and the solar cell parameters such as open circuit voltage (Voc), fill factor (FF), short circuit current density (Jsc) and power conversion efficiency (Eff).

The layer thickness is varied from 10 nm to 50 nm [70], the obtained results are shown in Figures 3.10 – 3.11 .

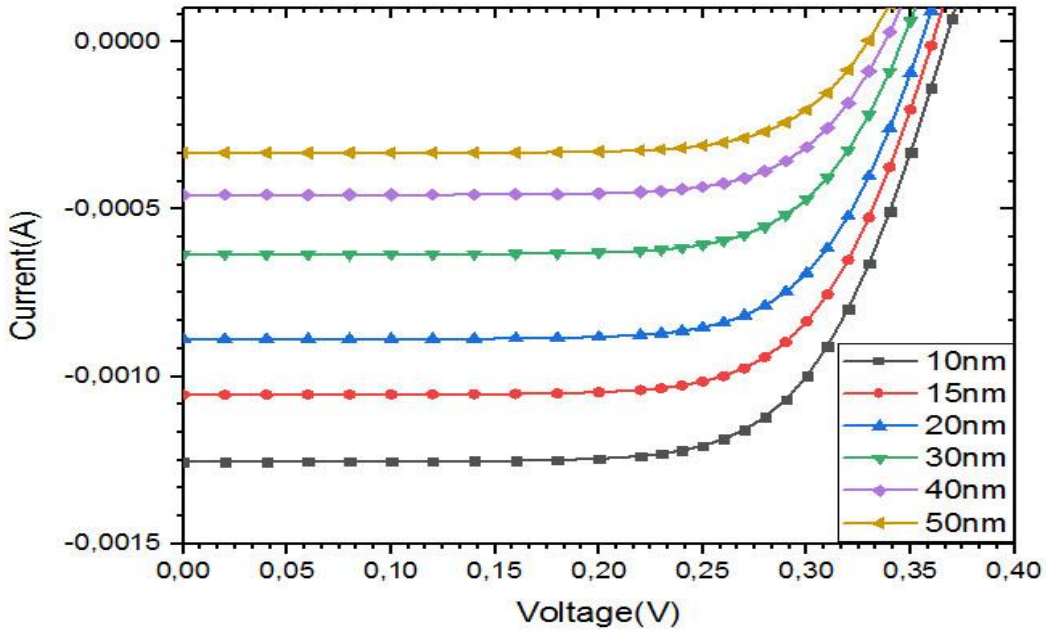

Figure3.10: Effect of graphene thickness on the J-V characteristic

Chapter 3 Results and discussion

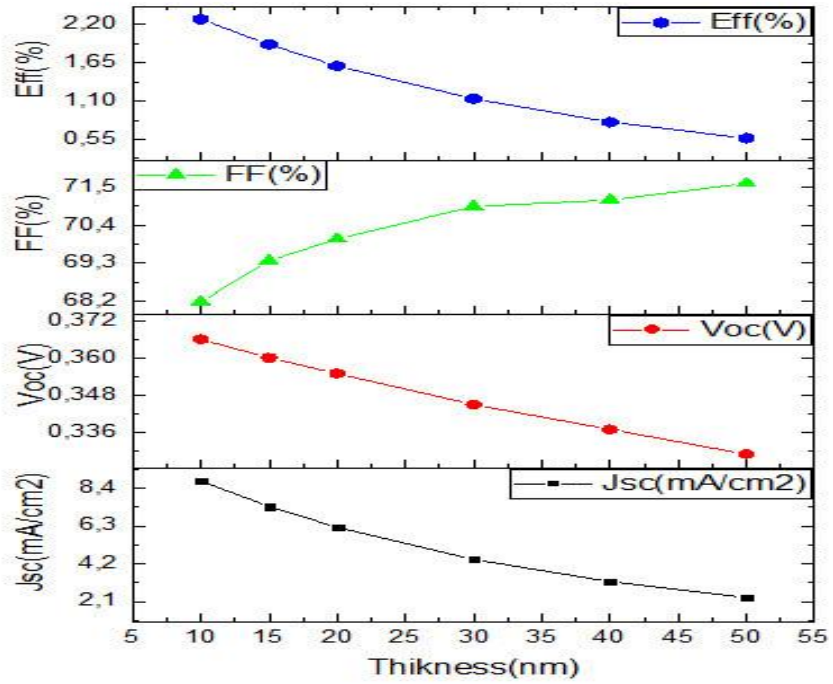

Figure 3.11: Effect of graphene thickness on the solar cell parameters

The current density (Jsc) decreases uniformly from 8.789 mA/cm^{-2} at 10 nm until 2.317 mA/cm^{-2} at 50 nm, While the (Voc) has a small changes between 0.36V and 0.33V. The (FF) has also a small increase from 68.18% to 71.61%, and the efficiency also decreased from 2.27% to 0.56%.

The decrease of (Jsc) is related to the decrease in the photocurrent, which in turn decreases with the decrease in transmission, this affects also the (Voc) which has a small change because of the logarithmic relation between Jsc and Voc as mentioned previously in equation 1.6.

The fill factor increases with the increasing of thickness maybe due to the decrease in series resistance which has an inverse relationship with the cross-section area of graphene.

Finally the efficiency is affected directly by the remarkable changes in short circuit current, so it behaves like it.

7.3. Effect of graphene oxide graphene/silicon solar cell

the effect of graphene oxide (GO) as an passivation interlayer between graphene and silicon on the J-V characteristic and parameters of the solar cells such as open circuit voltage (Voc), fill factor (FF), short circuit current density (Jsc) and power conversion efficiency (Eff) as shown in figure 3.12.

Chapter 3 Results and discussion

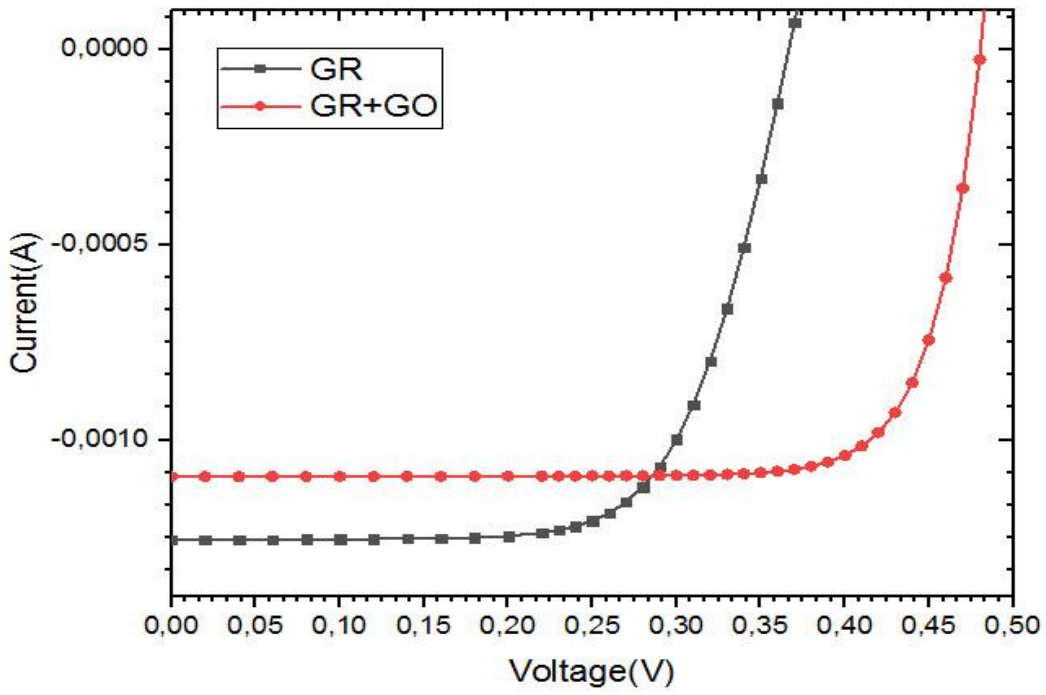

Figure 3.12: Effect of graphene oxide (GO) interlayer on the J-V characteristic

The (Voc) increase from $0.36V$ in graphene/silicon solar cell to 0.48V after adding GO, While The (Jsc) decrease from 8.78 mA/cm^{-2} to 7.66 mA/cm^{-2} And the efficiency also increase from 2.27% to 3.02% as shown in the table 3.2

Parameters	Jsc	Voc	FF	Eff
Gr/Si	8.78 mA/cm^{-2}	$0.36V$	68.18	2.27%
Gr/GO/Si	7.66 mA/cm^{-2}	0.48	79.22	3.02%

Table 3.3: Comparison between Gr/Si and Gr/GO/Si solar cells parameters

The increase of (Voc) is related directly with the GO band gap which have a large band gap (Eg=2.48 eV), On the other hand, the small change in (Jsc) is due to the increase in the GO forbidden gap compared to graphene's one, which leads to a loss of part of the free carriers generated by photons with energy less than the new forbidden gap. Finally, the efficiency increases because it is affected by the ratio of Jsc and Voc.where Voc increses by 33% while Jsc decreases by 13%.

7.4. Effect of doping concentration on solar cell

In this area we are going to consider the impact of Silicon doping on the J-V characteristic and parameters of the solar cells, open circuit voltage (Voc), fill factor (FF), short circuit current density (Jsc) and power conversion efficiency Eff.

Chapter 3 Results and discussion

In this case, the Silicon doping is varied from $1 \times 10^{15}\ cm^{-3}\ to\ 1 \times 10^{17}\ cm^{-3}$ as shown in figure 3.13-3.14.

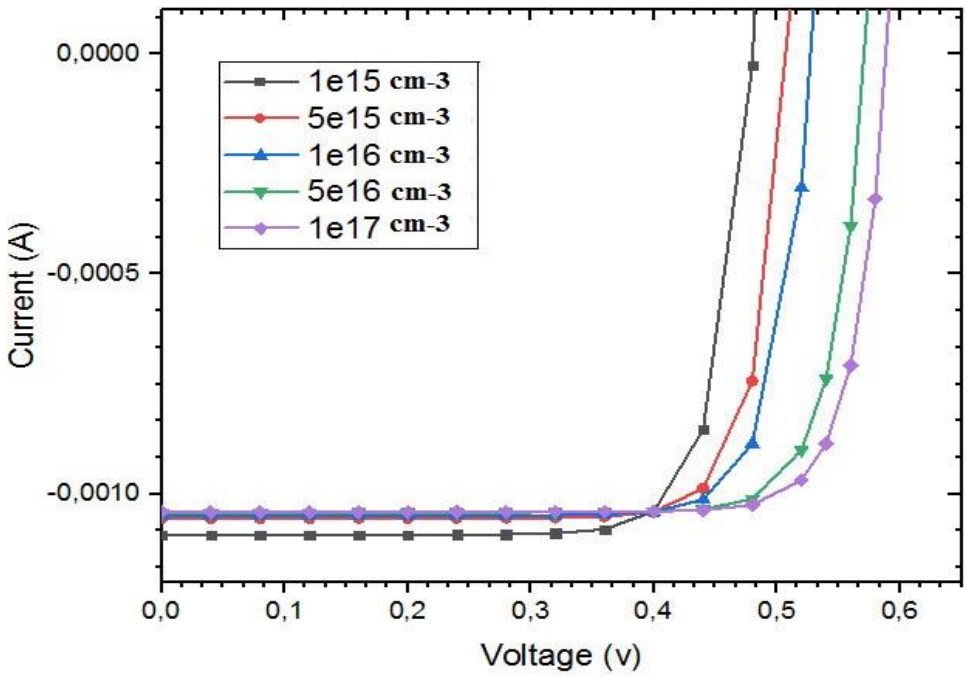

Figure 3.13: Effect of Silicon doping on the J-V characteristic

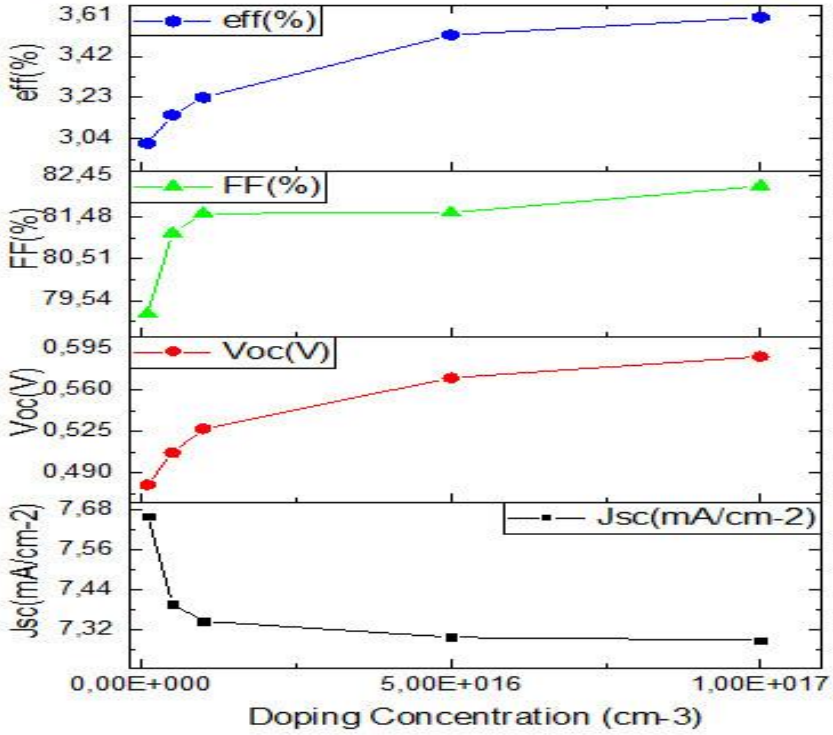

Figure 3.14: Effect of Silicon doping on the solar cell parameters

Chapter 3 Results and discussion

The (Voc) increase from 0.48 V at $1 \times 10^{15}\ cm^{-3}$ to 0.588V $1 \times 10^{17}\ cm^{-3}$,while the current density (Jsc) has a small change from 7.658 mA$/cm^{-2}$ to $7.289 mA/cm^{-2}$.

The (FF) slightly increases from 79.22% to 82.21% ,and the efficiency has also increased from 3.018% to 3.650%.

The (Voc) increase because it is related directly with the built in voltage and the last one has a direct relation with the doping concentration. Meanwhile, the (Jsc) small change may due to the shrinking depletion region by increasing doping effect.

Finally, the efficiency is affected directly by the significant change in the open circuit voltage (Voc), so it behaves like it.

7.5. Effect of SiO_2 on graphene/silicon solar cell

Now we will investigate the effect of SiO_2 also as passivation interlayer but this time between silicon and Anode on the J-V characteristic and parameters of the solar cells, open circuit voltage (Voc), fill factor (FF), short circuit current density (Jsc) and power conversion efficiency (Eff) as shown in figure 3.15.

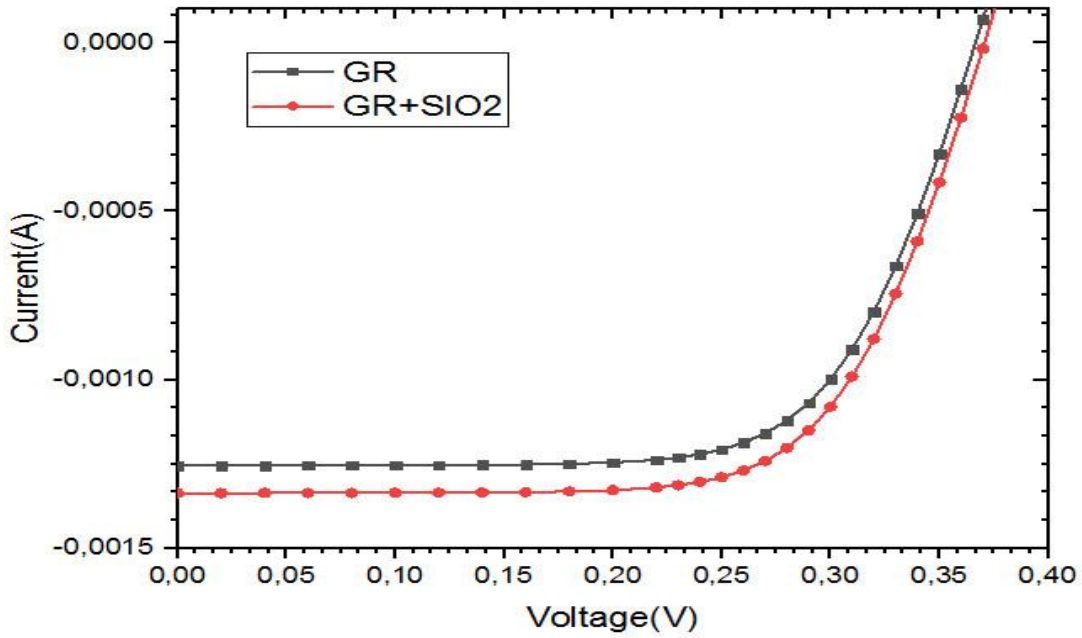

Figure3.15: Effect of SiO_2 interlayer on the J-V characteristic

The (Voc) has a small increase from 0.36V in graphene/silicon solar cell to 0.37 V after adding SiO_2, While the (Jsc) has considerable increase from 8.78 mA/cm^{-2} to 9.35 mA/cm^{-2}, and the efficiency also increase from 2.27% to 2.44%.

The (Jsc) has increased because of the presence of the passivation interlayer (SiO_2) barrier which blocks the holes and let the electrons pass by tunneling effect and also reduce the

surface defects so the recombination decrease and the Jsc increase, this change in Jsc affects also the (Voc) which has a small change because of the logarithmic relation between Jsc and Voc as mentioned above.

Finally, the efficiency increases because it is affected by the ratio of Jsc and Voc.

7.6. Effect of SiO_2 thickness on solar cell

In this section we are going to examine the impact of the SiO_2 layer thickness on the J-V characteristic and some parameters such as, open circuit voltage (Voc), fill factor (FF), short circuit current density (Jsc) and power conversion efficiency (Eff).The layer thickness is varied from 8 A to 20A.

The obtained results are shown in Figure 3.16 – 3.17 .

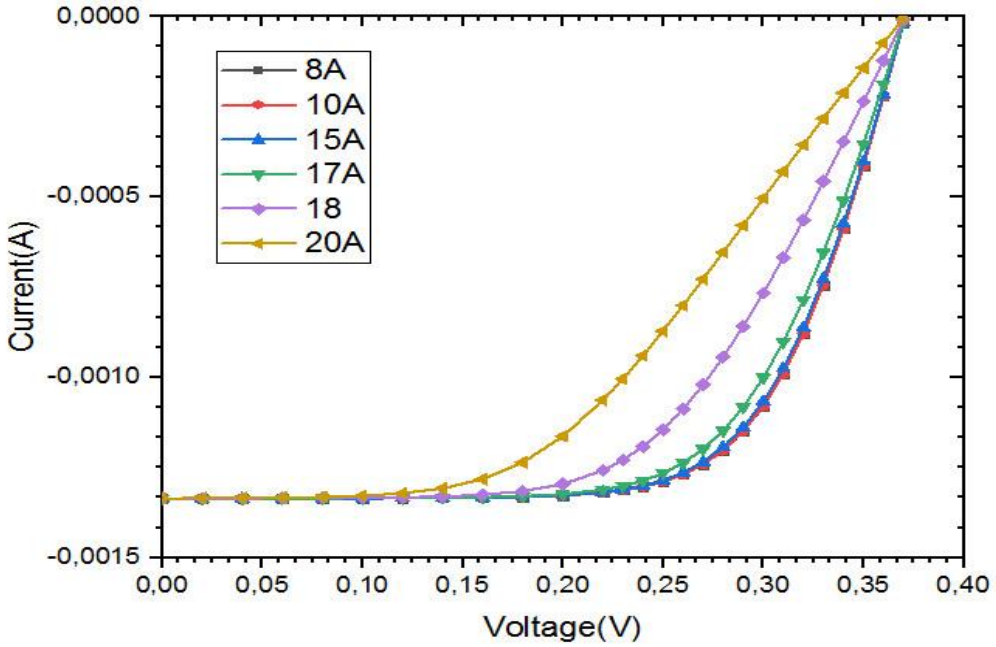

Figure3.16: Effect of SiO_2 thickness on the J-V characteristic

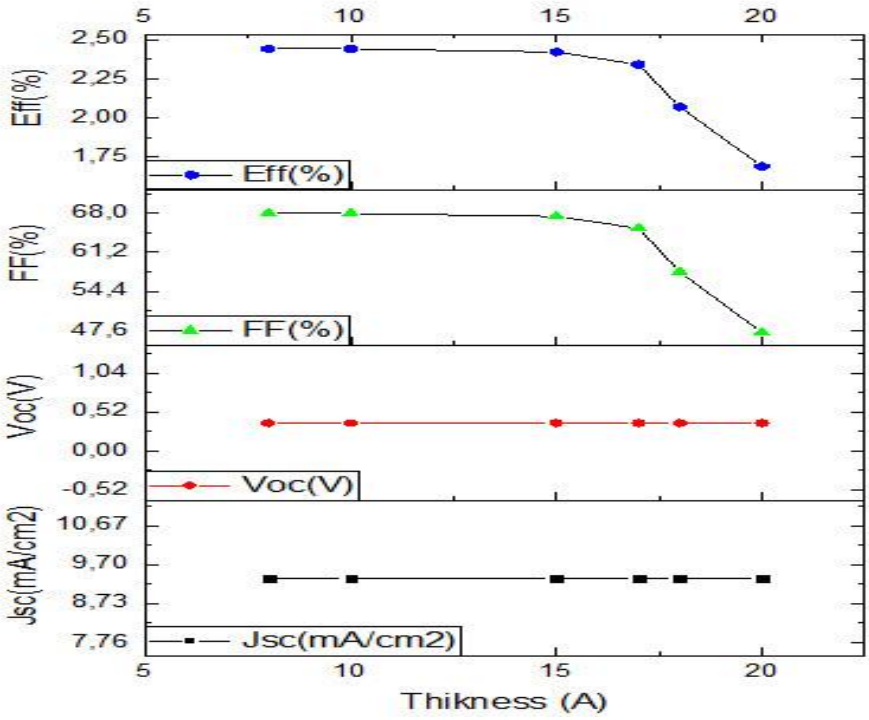

Figure 3.17: Effect of SiO_2 thickness on the solar cell parameters

the current density (Jsc) and the (Voc) doesn't changed, while the (FF) decrease from 67.95% to 47.23% and also the efficiency decreased from 2.44% to 1.69%.

these changes have relation with series resistance, the last one increase with the increase of the SiO_2 thickness which obstructs the passage of electrons by reducing the tunneling effect so the FF decrease and efficiency too .

7.7. Effect of all enhancements in one structure

Finally we will gather all the enhancements that we are studied above in one structure and see the effect of them combined on the J-V characteristic and the solar cell parameters such as open circuit voltage (Voc), fill factor (FF), short circuit current density (Jsc) and power conversion efficiency (Eff).

The obtained results are shown in figure 3.18 and table 3.4 .

Chapter 3 Results and discussion

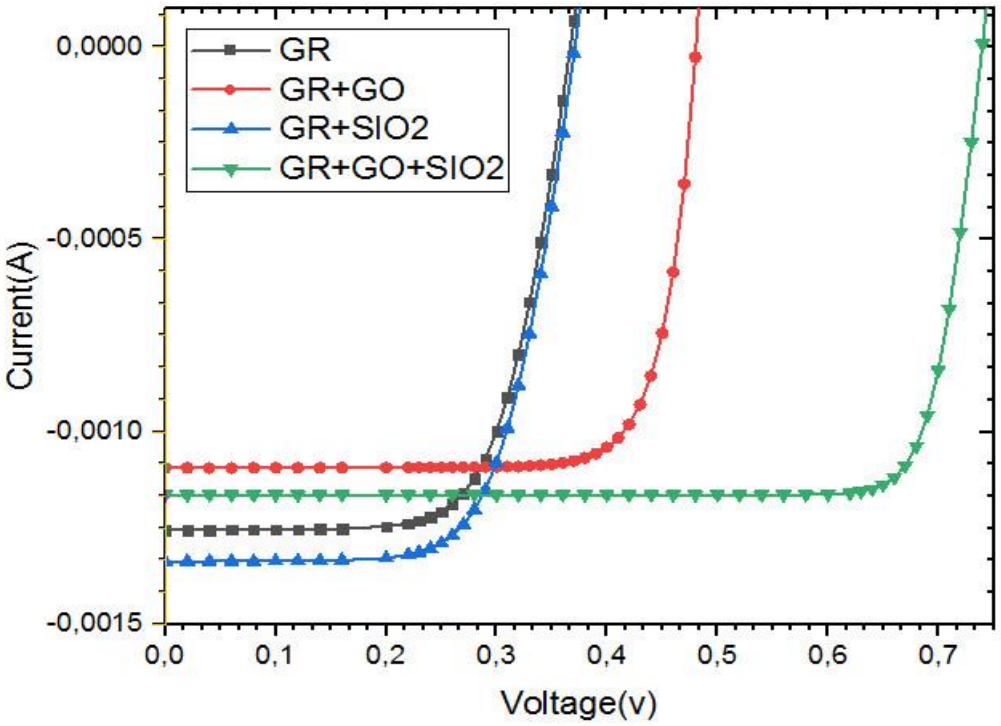

Figure 3.18: Comparison between I-V characteristic of studied solar cells (Gr/Si black, Gr/GO/Si red, passivated Gr/Si using SiO_2 layer blue, passivated Gr/GO/Si using SiO_2 layer green)

Parameters	$Jsc\ (mA/cm^{-2})$	$Voc(V)$	$FF(\%)$	$Eff(\%)$
Gr/Si	8.78	0.36	68.18	2.27
Gr/GO/Si	7.66	0.48	79.22	3.02
Gr/Si/SiO_2	9.35	0.37	67.94	2.44
Gr/GO/Si/SiO_2	8.14	0.74	85.92	5.36

Table 3.4: Parameters of studied solar cells

The final results summed up all the enhancement effect on the graphene/Si structure.

For example when we used the GO interlayer The (Voc) increase from $0.36\,V$ to $0.48\,V$ that's the direct cause why the efficiency increase from 2.27 % to 3.02% and when we add the SiO_2 interlayer the big effect was on the Jsc and it increase from $7.78\,mA/cm^{-2}$ to $9.35\,mA/cm^{-2}$ That's why the efficiency increase from 2.27 % to 2.44 %, and when we used them together in one structure Gr/GO/Si the efficiency improved a lot from 2.27 % to 5.36% because of the big increase of Voc from $0.36\,V$ to $0.74\,V$, this huge improvement was unexpected and its explanation requires more studies about this phenomenon.

Conclusion

Conclusion

In this work we have tried to both reducing the cost of silicon solar cells and improving the efficiency of such PV devices with studying the optimization of performance in graphene/Si solar cells because they can be one of the clean energy production in future.

The solar cell is studied via SILVACO ATLAS software simulations, to get the current-voltage characteristics and the Parameters of graphene/Si solar cell by studying some effects on this solar cell .

The simulation results show that depositing of interlayers can affect the solar cells efficiency, the insertion of GO and SiO_2 interlayers increases the efficiency from 2.27% to 3.02% and from 2.27% to 2.44% respectively and from 2.27% to 5.36% when we used them together in one structure in the best conditions , because it is related directly by the short circuit current Jsc and the open circuit voltage Voc, which in turn affects by the tunnel effect and the value of the band gap.

The simulation results show more additional importants parameters like the doping concentration and the thickness of the interlayers which affects the efficiency of the solar cell because it affects respectively the built in voltage and the resistance series.

References

[1] Energy Information Administration, International Energy Outlook 2013, EIA, 2013
[2] Alan Nanso; Nuclear energy - the future climate | The Royal Society,1999
[3] Luque, A.; Hegedus, S., Handbook of Photovoltaic Science and Engineering, John Wiley & Sons, 3 -312, 2003
[4] Comprehensive Renewable Energy, Ali Sayigh, Oxford Elsevier, 2012
[5] IEA-ETSAP and IRENA© Technology Brief E ll - January 2013
[6] Greenrhinoenergy.com, (2014). PV Cells & Modules, Photovoltaics | Solar Power, [online] Available at: http://www.greenrhinoenergy.com/solar/technologies/pv_modules.php
[7] ASTM Standard. G173, standard tables for reference solar spectral irradiances: Direct normal and hemispherical on 37 tilted surface. Annual book of ASTM standards, 12, 2008.
[8] Greg P Smestad. Optoelectronics of solar cells. SPIE press, 2002.
[9] Martin A Green. Solar cells: operating principles, technology, and system applications. 1982.
[10] Jean-Claude G Bunzli and Anne-Sophie Chauvin. Handbook on the Physics and Chemistry of Rare Earths, Elsevier, 2014.
Online on : https://www.sciencedirect.com/topics/physics-and-astronomy/solar-energy-conversion
[11] Energyplus. Weather data. from;
http:https://www.energy.gov/eere/buildings/downloads/energyplus-0
[12] PVGIS. Photovoltaic geographical information system-solar irradiation data. from; https://re.jrc.ec.europa.eu/pvg_tools/fr/
[13] John A. Du_e and William A. Beckman. Solar engineering of thermal processes. Wiley, fourth edition, 2013.
[14] Ali Mohammad Noorian, Isaac Moradi, and Gholam Ali Kamali. Evaluation of 12 models to estimate hourly diffuse irradiation on inclined surfaces. Renewable energy, 33(6):1406-1412, 2008.
[15] researchgate.net Online on : https://www.researchgate.net/figure/Distribution-of-average-global-solar-irradiance-for-every-hour-on-averaged-days-of_fig1_342407964
[16] Pveducation.org. Intrinsic Carrier Concentration | PVEducation. [online] Available at: https://www.pveducation.org/pvcdrom/pn-junctions/intrinsic-carrier-concentration
[17]Epa.gov. 2013. Future Climate Change | Climate Change | US EPA. [online] Available at: https://19january2017snapshot.epa.gov/climate-change-science/future-climate-change_.html#Greenhouse%20gas
[18] Pveducation.org. Solar Cell Structure | PVEducation. [online] Available at: http://pveducation.org/pvcdrom/solar-cell-operation/solar-cell-structure
[19] Pveducation.org. The photovoltaic effect | PVEducation. [online] Available at: https://www.pveducation.org/pvcdrom/solar-cell-operation/the-photovoltaic-effect
[20] Bjorn Petter Jelle, Christer Breivik, and Hilde Drolsum R_kenes. Building integrated photovoltaic products: A state-of-the-art review and future research opportunities. Solar Energy Materials and Solar Cells, 100:69-96, 2012.

References

[21] Martin A Green, Keith Emery, Yoshihiro Hishikawa, Wilhelm Warta, and Ewan D Dunlop. Solar cell efficiency tables (version 45). Progress in photovoltaics: research and applications, 23(1):1-9, 2015.
[22] AF Sherwani, JA Usmani, et al. Life cycle assessment of solar pv based electricity generation systems: A review. Renewable and Sustainable Energy Reviews, 14(1):540-544, 2010.
[23] NREL. Research Cell Efficiency Records. Available at : https://www.nrel.gov/pv/module-efficiency.html
[24] AL Fahrenbruch and RH Bube. Fundamentals of solar cells (academic, new york, 1983). Chap, 6:234-236.
[25] Chetan Singh Solanki. Solar photovoltaics: fundamentals, technologies and applications. PHI Learning Pvt. Ltd., 2015.
[26] Martin A Green. Photovoltaic principles. Physica E: Low-dimensional Systems and Nanostructures, 14(1):11-17, 2002.
[27] Nadja Rebecca Brun, Bernhard Wehrli, and Karl Fent. Ecotoxicological assessment of solar cell leachates: Copper indium gallium selenide (cigs) cells show higher activity than organic photovoltaic (opv) cells. Science of the Total Environment, 543:703-714, 2016.
[28] Varun Sivaram, Samuel D Stranks, and Henry J Snaith. Outshining silicon. Scientific American, 313(1):54-59, 2015.
[29] Tom Markvart and Luis Castaner. Solar cells: materials, manufacture and operation. Elsevier, 2004.
[30] Tetsuo Soga. Nanostructured materials for solar energy conversion. Elsevier, 2006.
[31] Marco Ficcadenti and Roberto Murri. Basics of thin film solar cells. 2013.
[32] Sameer Chhajed, Martin F Schubert, Jong Kyu Kim, and E Fred Schubert. Nanostructured multilayer graded-index antireection coating for si solar cells with broadband and omnidirectional characteristics. Applied Physics Letters, 93(25):251108, 2008.
[33] Jenny Nelson. The physics of solar cells, volume 1. World Scienti_c, 2003.
[34] Afshin Izadian, Arash Pourtaherian, and Sarasadat Motahari. Basic model and governing equation of solar cells used in power and control applications. In Proc. IEEE Energy Convers. Expo. Conf, pages 1483-1488, 2012.
[35] Cristina Cornaro and Angelo Andreotti. Influence of average photon energy index on solar irradiance characteristics and outdoor performance of photovoltaic modules. Progress in Photovoltaics: Research and Applications, 21(5):1002,2012.
[36] Claudia Strumpel, Michelle McCann, Guy Beaucarne, Vladimir Arkhipov, Abdelilah Slaoui, V .Svrcek, C Del Canizo, and I Tobias. Modifying the solar spectrum to enhance silicon solar cell efficiency an overview of available materials. Solar Energy Materials and Solar Cells, 91(4):238-249, 2007.
[37] Thomas Huld, Gabi Friesen, Artur Skoczek, Robert P Kenny, Tony Sample, Michael Field, and Ewan D Dunlop. A power-rating model for crystalline silicon pv modules. Solar Energy Materials and Solar Cells, 95(12):3359-3369, 2011.

References

[38] Michael Koehl, Markus Heck, Stefan Wiesmeier, and Jochen Wirth. Modeling of the nominal operating cell temperature based on outdoor weathering. Solar Energy Materials and Solar Cells, 95(7):1638-1646, 2011.

[39] N Martin and JM Ruiz. Calculation of the pv modules angular losses under field conditions by means of an analytical model. Solar Energy Materials and Solar Cells, 70(1):25-38, 2001.

[40] Thomas Huld, Marcel Suri, and Ewan D Dunlop. Comparison of potential solar electricity output from fixed-inclined and two-axis tracking photovoltaic modules in europe. Progress in photovoltaics: Research and Applications, 16(1):47-59, 2008.

[41] Steven Magee. Solar Irradiance and Insolation for Power Systems. Steven Magee, 2010.

[42] Minnaert, B., & Veelaert, P. (2014). A proposal for typical artificial light sources for the characterization of indoor photovoltaic applications. *Energies*, *7*(3), 1500-1516.

[43] Choi, W., & Lee, J. W. (Eds.). (2011). Graphene: synthesis and applications. CRC press.

[44] Jr, W. H. & Offeman, R. Preparation of graphitic oxide. Journal of the American Chemical Society 208, 1937 (1958)

[45] Stoller, M.D.; Park, S.; Zhu, Y.; An, J.; Ruoff, R.S.: "Graphene-Based Ultracapacitors". Nano Letters, 2008, 8, 3498-3502.

[46] Novoselov, K.S.; Jiang, D.; Schedin, F.; Booth, T.J.; Khotkevich, V.V.; Morozov, S.V.; Geim, A.K.: "Two-Dimensional Atomic Crystals". Proceedings of the National Academy of Sciences of the United States of America, 2005, 102, 10451-10453.

[47] Harrison, B.S.; Atala, A.: "Carbon Nanotube Applications for Tissue Engineering". Biomaterials, 2007, 28, 344-353.

[48] Berger, C.; Song, Z.; Li, X.; Wu, X.; Brown, N.; Naud, C.; Mayou, D.; Li, T.; Hass, J.; Marchenkov, A.N.; Conrad, E.H.; First, P.N.; de Heer, W.A.: "Electronic Confinement and Coherence in Patterned Epitaxial Graphene". Science, 2006, 312, 1191-1196.

[49] Li, D.; Muller, M.B.; Gilje, S.; Kaner, R.B.; Wallace, G.G.: "Processable Aqueous Dispersions of Graphene Nanosheets". Nature Nanotechnology, 2008, 3, 101-105

[50] Wang, X.; Zhi, L.J.; Mullen, K.: "Transparent, Conductive Graphene Electrodes for Dye-Sensitized Solar Cells". Nano Letters, 2008, 8, 323-327.

[51] Avouris, P. Graphene: Electronic and photonic properties and devices. Nano Letters 10, 4285–4294 (2010).

[52] Balandin, A. A. Thermal properties of graphene and nanostructured carbon materials. Nature Materials 10, 569–581 (2011).

[53] Gilje, S. et al. Photothermal Deoxygenation of Graphene Oxide for Patterning and Distributed Ignition Applications. Advanced Materials 22, 419–423 (2010).

[54]Song, E. B. et al. Visibility and Raman spectroscopy of mono and bilayer graphene on crystalline silicon. Applied Physics Letters 96, 81911 (2010).

[55]Nair, R. R. et al. Fine structure constant defines visual transparency of graphene. Science 320, 1308 (2008).

[56] Stoller, M. D., Park, S., Zhu, Y., An, J. & Ruoff, R. S. Graphene-Based Ultracapacitors. Nano Letters 8, 3498–3502 (2008)

[57] Merlet, C., Rotenberg, B., Madden, P. & Taberna…, P. On the molecular origin of supercapacitance in nanoporous carbon electrodes. Nat Materials (2012).

[58] Hummers Jr, William S., and Richard E. Offeman. "Preparation of graphitic oxide." *Journal of the American Chemical Society* 80, no. 6 (1958): 1339-1339.

References

[59] Thema, F. T., M. J. Moloto, E. D. Dikio, N. N. Nyangiwe, L. Kotsedi, M. Maaza, and M. Khenfouch. "Synthesis and characterization of graphene thin films by chemical reduction of exfoliated and intercalated graphite oxide."*Journal of chemistry* 2013 (2012).
[60] Pei, Songfeng, and Hui-Ming Cheng. "The reduction of graphene oxide." *Carbon*50, no. 9 (2012): 3210-3228.
[61] A. Goetzberger, J. Knobloch, and B. VoB, "Si Solar Cell Technology," in *Crystalline Silicon Solar Cells*.: John Wiley & Sons, 1998, pp. 133-162.
[62] I. Tarasov, *Defect diagnostic using scanning photoluminescence in multicrystalline silicon for solar cells*. Tampa, Fl: University of South Florida, 2002.
[63] F. Ferrazza, "Crystalline silicon: Manufacture and properties," in *Solar Cells: Materials, Manufacture And Operation*. Oxford, UK: Elsevier, 2005, pp. 72-87.
[64] W. Koch et al., "Bulk Crystal Growth and Wafering for PV," in *Handbook of photovoltaic science and engineering*, A. Luque and S. Hegedeus, Eds. Chichester, UK: Wiley, 2003, ch. 6, pp. 205-254.
[65] E. A. Schiff and X. Deng, "Amorphous silicon–based solar cells," in *Handbook of photovoltaic science and engineering*, A. Luque and S. Hegedeus , Eds. Oxford, UK: Wiley, 2003, ch. 12, pp. 505-566.
[66] Tilli, M., & Haapalinna, A. (2020). Properties of silicon. In *Handbook of Silicon Based MEMS Materials and Technologies* (pp. 3-4). Elsevier.
[67]Silvaco, I. (2018). ATLAS user's manual device simulation software. *Santa Clara, CA*.
[68]Yang, L., Yu, X., Xu, M., Chen, H., & Yang, D. (2014). Interface engineering for efficient and stable chemical-doping-free graphene-on-silicon solar cells by introducing a graphene oxide interlayer. Journal of Materials Chemistry A, 2(40), 16877-16883.
[69] Chenaf Kaouther.,Study of graphene-based solar cells by simulation
[70]Li, X., et al., *Graphene-on-silicon Schottky junction solar cells.* 2010. 22(25): p. 2743-2748.